

Coupled Electron-Ion Monte Carlo of high pressure hydrogen

Carlo Pierleoni

Physics Department, University of L'Aquila, Italy

● Collaborations

- David M. Ceperley, UIUC, Illinois USA
- Kris Delaney, UCSB, California USA.
- Markus Holzmann, LPTCM, Paris VI, France.
- Miguel Morales, UIUC, Illinois USA

● Acknowledgments

INFM and PRIN 2001-2003-2005 for financial support
CECAM for his hospitality
NCSA (USA) and CINECA (Italy) for computer time.

Outline

- Motivations
 - Beyond DFT
 - High pressure hydrogen: phase diagram and MIT
- Coupled Electron-Ion Monte Carlo (CEIMC)
 - Finite temperature Ions: Noisy Monte Carlo **The Penalty Method**
 - Ground state electrons:
 - VMC & RQMC
 - Trial wave functions for hydrogen
 - Energy difference methods
 - Finite size effects: Twist Average Boundary Conditions (TABC)
 - Moving the electrons: **the bounce algorithm**
 - Strategy for Protonic PIMC within CEIMC
- Application: High pressure hydrogen
- Future developments

motivations: beyond DFT

- Modern *AB-INITIO* simulation methods are largely based on Density Functional Theory (DFT), in principle exact but in practice it invokes the Local Density Approximation (LDA and various improvements GGA).
- DFT+LDA(GGA) is in general a good compromise between accuracy and efficiency to perform **dynamical** studies of several hundreds atoms for times of the order of *100 psec* (Car-Parrinello and BO Molecular Dynamics).
- There are cases in which DFT is not accurate enough (Van-der-Waals bonding systems, sp-bonded materials, calculation of excitation energies and energy gaps)
- Can we do better than DFT? **Quantum Monte Carlo (QMC)** provides in general better electronic energies for given ionic positions.

beyond DFT

- Can we devise an efficient method to exploit the accuracy of QMC in *AB-INITIO* "dynamical" simulation of condensed systems?

beyond DFT

- Can we devise an efficient method to exploit the accuracy of QMC in *AB-INITIO* "dynamical" simulation of condensed systems?
- Previous attempts
 - Diffusion Monte Carlo for electrons and nuclei (DMC) (Ceperley-Alder 1987)
 - temperature effects are absent
 - time scale separation problem (even for hydrogen!)
 - Restricted Path Integral Monte Carlo (RPIMC) (Pierleoni et al, 1994, Militzer & Ceperley 1999)
 - electrons and nuclei are at finite temperature
 - sampling problem at low temperature ($T < 1/20T_F$)

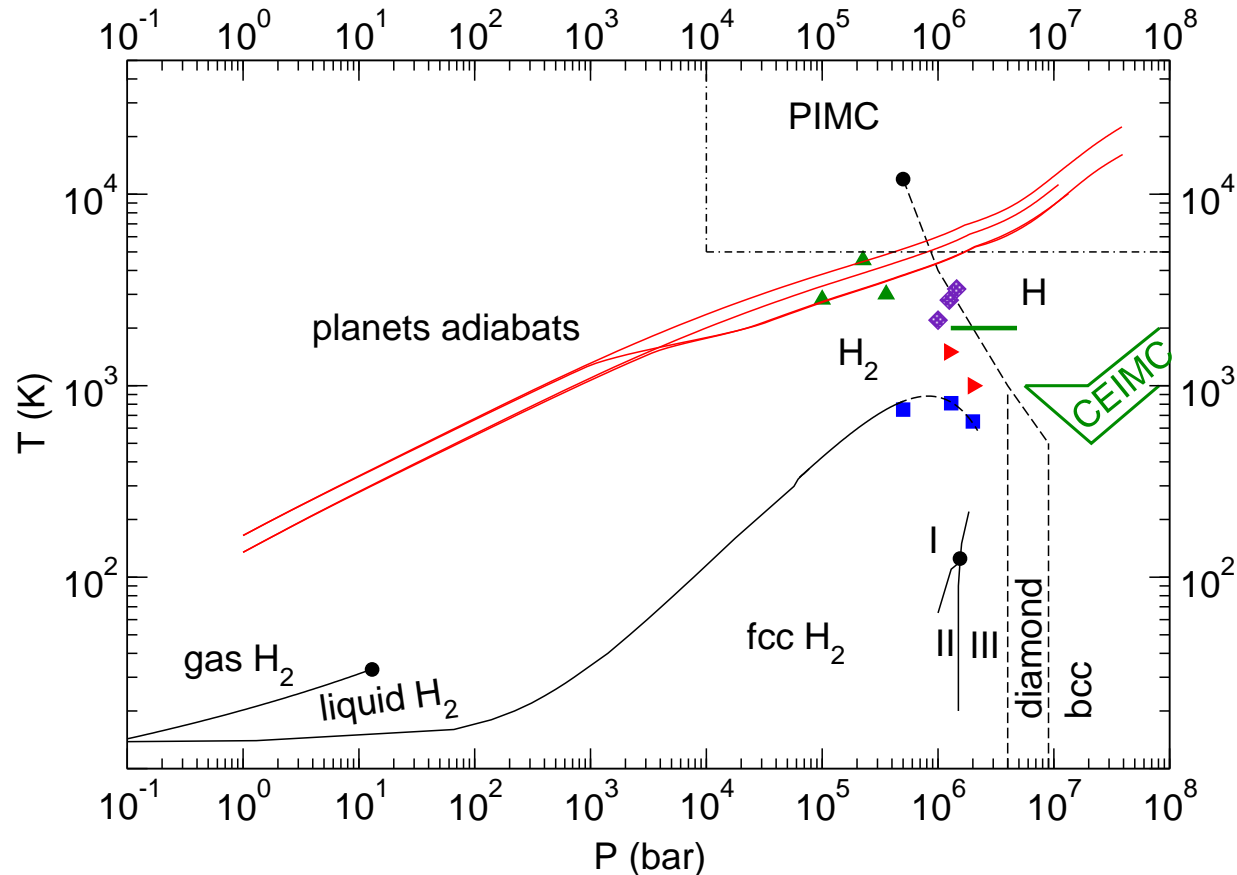
beyond DFT

- Can we devise an efficient method to exploit the accuracy of QMC in *AB-INITIO* "dynamical" simulation of condensed systems?
- Previous attempts
 - Diffusion Monte Carlo for electrons and nuclei (DMC) (Ceperley-Alder 1987)
 - temperature effects are absent
 - time scale separation problem (even for hydrogen!)
 - Restricted Path Integral Monte Carlo (RPIMC) (Pierleoni et al, 1994, Militzer & Ceperley 1999)
 - electrons and nuclei are at finite temperature
 - sampling problem at low temperature ($T < 1/20T_F$)
- **Coupled Electron-Ion Monte Carlo (CEIMC)**
 - Born-Oppenheimer separation of time scales:
ground state electrons, finite T nuclei

High pressure hydrogen

- The most abundant element in the universe : giant planets (>90%)
- The simplest element in the periodic table: good theoretical playground
- Still so much unknown!! The high pressure phases are still largely out of the experimental reach.

Hydrogen: phase diagram



Continuous transition lines (in black): experimental results

dashed lines: theoretical prediction from various methods

red lines: model adiabats for the interior of the giant planets of the solar system

diamonds: shock-waves experiments through liquid metalization (Weir et al. PRB '96)

squares: CPMD predictions of molecular melting (Bonev et al, Nature '04)

right-triangle: CPMD predictions for molecular dissociation in the liquid phase (Scandolo, PNAS '03).

in green: CEIMC predictions

Hydrogen: know facts

- Solid hydrogen is insulating up to 3.5Mbars (DAC experiments, Loubeyre Nature '02)
- at T=0K molecular dissociation occurs at $r_s=1.31$ (DMC, Ceperley Alder PRB '87)
- At the molecular dissociation a diamond structure of protons is predicted. At higher pressure a diamond–bcc transition is expected (DMC, Natoli et al PRL '93).
- crystal structures of different symmetry can have very close energies: needs of very accurate total energy methods.
- Size effects are crucial to obtain accurate energies (Brillouin zone sampling in CPMD).
- ZPM is large and favors isotropic structures (Kitamura et al, Nature 2000).
- Molecular phases I and II are understood, phase III is still unsettled.
- Predicting metalization requires going beyond DFT-LDA-GGA (Johnson Ashcroft, Nature 2000)
- Most recent prediction (T=0K): $P_c \simeq 4$ Mbars within the molecular phase (DFT-Exact-Exchange functional) (Stadele and Martin, PRL 2000). But this method is too demanding to be used in a "dynamical" simulation.
- Molecular-atomic (insulating-metallic) transition in the liquid at higher temperature (T=1500K) has been recently predicted by CPMD (Scandolo, PNAS 2003) but not yet confirmed by experiments. At higher T ($\simeq 5000$ K) PIMC exhibits a continuous molecular-atomic transition.

CEIMC

CEIMC: Metropolis Monte Carlo for the finite T ions. The BO energy in the Boltzmann distribution is obtained by a QMC calculation for the ground state electrons.

- Finite temperature ions: Noisy Monte Carlo **The Penalty Method**
- Ground state electrons:
 - VMC & RQMC
 - Trial wave functions for hydrogen
 - Energy difference methods
 - Finite size effects: Twist Average Boundary Conditions (TABC) within CEIMC
 - Moving the electrons: **the bounce algorithm**
- Pre-rejecting protonic moves: multilevel Metropolis
- Strategy for Protonic PIMC within CEIMC

Moving the ions

- In Metropolis MC we generate a Markov chain of ionic states S distributed according to Boltzmann

$$P(S) \propto \exp(-\beta E_{BO}(S))$$

$E_{BO}(S)$ = Born-Oppenheimer energy for the configuration S .

- Given an initial state S we propose a trial state S' with probability

$$T(S \rightarrow S') = T(S' \rightarrow S)$$

and we accept the move with probability

$$A(S \rightarrow S') = \min [1, \exp \{-\beta [E_{BO}(S') - E_{BO}(S)]\}]$$

- After a finite number of moves the Markov chain is distributed with Boltzmann (if ergodicity holds).
- But $E_{BO}(S)$ from QMC is noisy \Rightarrow use the penalty method

The Penalty Method

- Assume mean value and variance of the energy difference over the noise distribution $P(\delta|S, S')$ exist

$$\begin{aligned}\beta[E_{BO}(S') - E_{BO}(S)] &= \langle \delta(S, S') \rangle = \Delta(S, S') \\ \langle (\delta - \Delta)^2 \rangle &= \sigma^2(S, S')\end{aligned}$$

We want to find the new acceptance probability $a(S \rightarrow S')$ such that **we satisfy detailed balance on average**:

$$T(S \rightarrow S') \langle a(S \rightarrow S') \rangle = T(S' \rightarrow S) \langle a(S' \rightarrow S) \rangle \exp[-\beta\Delta(S, S')]$$

$$\langle a(S \rightarrow S') \rangle = \int_{-\infty}^{\infty} d\delta P(\delta|S, S') a(\delta|S, S')$$

Under general assumption one can show that

$$a(\delta|\sigma) = \min \left[1, \exp \left(-\delta - \frac{\sigma^2}{2} \right) \right]$$

- The noise always causes extra rejection !**

The Penalty Method

- **EFFICIENCY**: which level of noise is optimal?

For a generic observable we ask which level of noise minimizes its statistical error ϵ^2 at

fixed computer time T : $T = m[nt + t_0]$

m =total number of ionic steps attempted

n =number of electronic calculations before the acceptance test

t =CPU time for a single electronic calculation

t_0 =time in the noiseless part of the code per total step

In general $\epsilon = c(s)m^{-(1/2)}$ and $s = \sigma n^{-(1/2)}$. ($c(s)$ and σ are unknown).

A measure of the inefficiency of our calculation is:

$$T\epsilon^2 = c^2(s)t_0 \left[1 + \frac{f}{s^2} \right] \quad f = \sigma^2 \frac{t}{t_0}$$

For any given application we have to choose s which minimize this quantity.

- In few simple examples the **optimal noise level** was found to be $s^2 = \sigma^2/n \approx 1$.

In CEIMC other constraints impose the noise level but as a rule of thumb we always try to stay around 1.

- $\sigma^2 \sim T^{-2}$: lowering the temperature requires smaller noise level, i.e. longer electronic runs

The electronic problem

System of N_p ions and N_e electrons. We need to compute the BO energy

$$E_{BO}(S) = \langle \Phi_0(S) | \hat{H} | \Phi_0(S) \rangle$$

$|\Phi_0(S)\rangle =$ electronic ground state w.f. for ionic state $S = \{\vec{s}_1, \dots, \vec{s}_{N_p}\}$.

In configurational space $X = (R, \Sigma) = (\{r_1, \dots, r_{N_e}\}, \{\sigma_1, \dots, \sigma_{N_e}\})$

$$E_{BO}(S) = \int dX |\Phi_0(X|S)|^2 E_L(X|S); \quad E_L(X|S) = \frac{\hat{H}(R, S)\Phi_0(X|S)}{\Phi_0(X|S)}$$
$$\sigma^2(S) = \int dX |\Phi_0(X|S)|^2 [(E_L(X|S) - E_{BO}(S))]^2$$

The electronic problem

System of N_p ions and N_e electrons. We need to compute the BO energy

$$E_{BO}(S) = \langle \Phi_0(S) | \hat{H} | \Phi_0(S) \rangle$$

$|\Phi_0(S)\rangle =$ electronic ground state w.f. for ionic state $S = \{\vec{s}_1, \dots, \vec{s}_{N_p}\}$.

In configurational space $X = (R, \Sigma) = (\{r_1, \dots, r_{N_e}\}, \{\sigma_1, \dots, \sigma_{N_e}\})$

$$E_{BO}(S) = \int dX |\Phi_0(X|S)|^2 E_L(X|S); \quad E_L(X|S) = \frac{\hat{H}(R, S)\Phi_0(X|S)}{\Phi_0(X|S)}$$

$$\sigma^2(S) = \int dX |\Phi_0(X|S)|^2 [(E_L(X|S) - E_{BO}(S))]^2$$

● If $|\Phi_0(S)\rangle$ is an eigenfunction of \hat{H}

$$\begin{cases} E_L(X|S) & = E_{BO}(S) \\ \sigma^2(S) & = 0 \end{cases} \quad \text{zero variance principle}$$

Variational Monte Carlo - VMC 1

- The “Variational Theorem”: assume a trial wave function for the electrons in the external field of the ions $\Psi_T(X|S)$ and compute the total energy as the average of the local energy $E_L = \Psi_T^{-1} H \Psi_T$

$$E_0 \leq E_T = \frac{\langle \Psi_T | \hat{H} | \Psi_T \rangle}{\langle \Psi_T | \Psi_T \rangle} = \frac{\int dX |\Psi_T(X; S)|^2 \Psi_T^{-1}(X; S) \hat{H} \Psi_T(X; S)}{\int dX |\Psi_T(X; S)|^2}$$

- The functional form of the trial wave function must be **suitable**
 - continuous
 - of proper symmetry
 - normalizable
 - **with finite variance** (for MC only)
- Parametrized: for a given functional form Ψ_T depends on a number of parameters $\vec{\alpha} = (\alpha_1, \dots, \alpha_n)$

$$\Psi_T(X|S, \vec{\alpha}) \implies E_T(S, \vec{\alpha}) = \langle E_L(X|S, \vec{\alpha}) \rangle$$

VMC 2

1. Since $|\Psi_T|^2 \geq 0$, VMC uses Metropolis MC to sample $P(X|S, \alpha) = |\Psi_T|^2 / \int dr |\Psi_T|^2$.
 2. take averages of the local energy and the variance
 3. optimize over $\{\alpha_i\}$ by minimizing energy and/or variance
 4. repeat until convergence is reached
- in CEIMC VMC-optimization should be done for each protonic configuration:
major bottleneck for the method
 - possible solutions
 - use an automatic optimization method such as Projection MC
 - in special cases use trial wave functions without variational parameters
(mono-atomic metallic hydrogen)

Reptation QMC: RQMC-1

Assume a trial state $|\Psi_T\rangle$

$$|\Psi_T\rangle = \sum_i c_i |\Phi_i\rangle \longleftarrow \text{eigenstates of } \hat{H}$$

$$|\Psi(t)\rangle \equiv e^{-t\hat{H}}|\Psi_T\rangle = \sum_i c_i e^{-tE_i} |\Phi_i\rangle \implies \lim_{t \rightarrow \infty} |\Psi(t)\rangle \propto |\Phi_0\rangle$$

$$E_0 = \frac{\langle \Phi_0 | \hat{H} | \Phi_0 \rangle}{\langle \Phi_0 | \Phi_0 \rangle} = \lim_{t \rightarrow \infty} \left\{ E(t) = \frac{\langle \Psi(t/2) | \hat{H} | \Psi(t/2) \rangle}{\langle \Psi(t/2) | \Psi(t/2) \rangle} = \frac{\langle \Psi_T | e^{-\frac{t}{2}\hat{H}} \hat{H} e^{-\frac{t}{2}\hat{H}} | \Psi_T \rangle}{\langle \Psi_T | e^{-t\hat{H}} | \Psi_T \rangle} \right\}$$

Define the generating function of the moments

$$Z(t) = \langle \Psi_T | e^{-t\hat{H}} | \Psi_T \rangle \implies \begin{cases} E(t) = -\partial_t \log Z(t) = \langle E_L \rangle_t & \longrightarrow E_0 \\ & t \rightarrow \infty \\ \sigma^2(t) = \partial_t^2 \log Z(t) = -\partial_t E(t) > 0 & \longrightarrow 0 \end{cases}$$

- The energy converges monotonously from above ($\partial_t E(t) \leq 0$)
- At any finite time t , $E(t)$ is a variational upper bound to E_0 : $E(t) \geq E_0$

RQMC - 2

In configuration space

$$Z(t) = \int dR dR' \langle \Psi_T | R \rangle \rho(R, R', t) \langle R' | \Psi_T \rangle$$

$\rho(R, R', t) = \langle R | e^{-t\hat{H}} | R' \rangle$ is the thermal density matrix at inverse temperature t .

Factorization ($t = M\tau$) \implies path integral

$$\rho(R, R', t) = \langle R | (e^{-\tau\hat{H}})^M | R' \rangle = \int dR_1 \cdots dR_{M-1} \prod_{k=1}^{M-1} \rho(R_{k-1}, R_k, \tau)$$

$R_0 = R, R_M = R'$ paths boundary conditions in imaginary time

Importance sampling

$$Z(t) = \int dR dR' \Psi_T(R) \left\langle e^{-\int_0^t d\tau E_L(R(\tau))} \right\rangle_{DRW} \Psi_T(R')$$

Summary of FN-RQMC

- Build a path $Q = (R_0, \dots, R_M)$ for the system of N_e electrons at fixed ionic configuration S .
- Sample the path space according to the distribution

$$\mathbf{\Pi}(Q|S) = \exp [- U(R_0|S) - U(R_M|S) - A(Q|S)]$$

$$U(R|S) = \Re[\ln \Psi_T(R|S)]$$

$$A(Q|S) = \text{path action}$$

- **FN:** check $\Psi_T(R_{k-1})\Psi_T(R_k) > 0$ along the path. Otherwise reject the new path.
- Compute the local energy and the variance at path ends, other properties at the **middle**:

$$O(t) = \frac{1}{Z(t)} \int dR_1 dR_2 dR_3 \Psi_T^*(R_1) \rho(R_1, R_2 | \frac{t}{2}) \langle R_2 | \hat{O} | R_2 \rangle \rho(R_2, R_3 | \frac{t}{2}) \Psi_T(R_3)$$

no mixed estimators bias!!!

- ensure convergence to the continuum limit ($\tau \rightarrow 0$) and to the ground state ($t \rightarrow \infty$)

Trial wave functions: $|\Psi_T\rangle$

- Slater-Jastrow form

$$\Psi_T(R|S) = \exp[-U(R|S)] \text{Det}(\Sigma^\uparrow) \text{Det}(\Sigma^\downarrow)$$

- $U(R)$ is a (two-body + three-body + ...) correlation factor ("pseudopotential")
- Σ^\uparrow is a Slater determinant of single electron orbitals $\theta_k(\vec{x}_i, \sigma_i|S)$.
- The nodes are determined by the form of the orbitals only. They are the most important part of the trial function since the nodes are not optimized by projection.

Dense hydrogen: more later !!!

Energy difference method

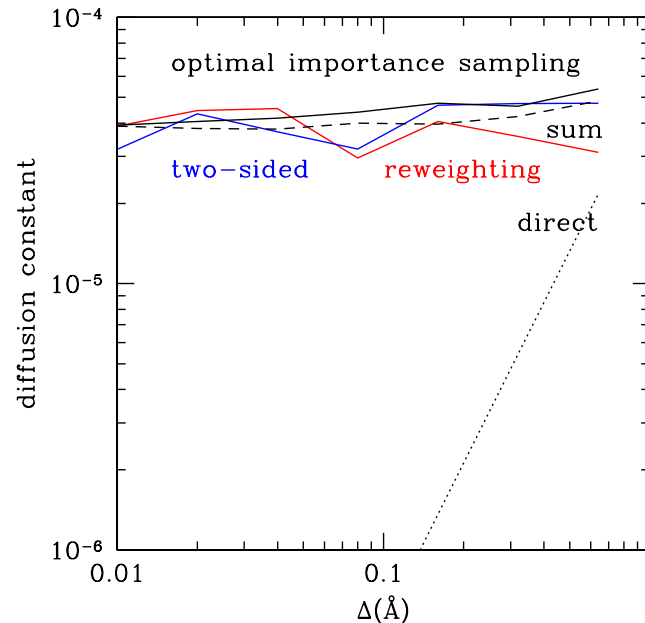
- In CEIMC we need to evaluate the energy difference between two closeby protonic configurations (S,S').
- Two independent electronic calculations (uncorrelated sampling) is very inefficient for $\Delta E \ll E$.
- Optimal sampling function: minimizes the variance of the energy difference

$$P(Q|S, S') \propto |\Pi(Q|S)(E_S - \langle E_S \rangle) - \Pi(Q|S')(E_{S'} - \langle E_{S'} \rangle)|$$

but it requires an estimate of $\langle E_S \rangle, \langle E_{S'} \rangle$.

- **simpler form:** $P(Q|S, S') \propto \Pi(Q|S) + \Pi(Q|S')$
- These two forms have the properties that
 - sample regions of both configuration spaces (S and S')
 - make the energy difference bounded
- compute properties for the system S by reweighting technique (RQMC easier than DMC).

Energy difference method



Efficiency versus importance function on a system with $N_e = N_p = 16$ and $r_s = 1.31$. In one system the protons are taken in a simple cubic lattice and in the other they are displaced randomly, with an average displacement of Δ . The diffusion constant is defined as Δ^2/T_{CPU} where T_{CPU} is the computer time needed to calculate the energy difference to an accuracy of 1000 K .

Finite size effects: TABC

- In the metallic systems finite size effects coming from the discrete structure of the Fermi surface are dominant and must be carefully treated.

The finite size effects can be reduced to the classical $1/N$ behavior averaging over the undetermined phase of the wave function (Li et al. PRE 2001). For periodic systems we have

$$\Psi(\vec{r}_1 + L\hat{x}, \vec{r}_2, \dots) = e^{i\theta_x} \Psi(\vec{r}_1, \vec{r}_2, \dots) \quad \theta \in [-\pi, \pi)$$

TABC:

$$A = \frac{1}{(2\pi)^3} \int_{-\pi}^{\pi} d^3\theta \langle \Psi_\theta | A | \Psi_\theta \rangle$$

- In practice θ can be chosen on a 3D grid and independent calculations are performed for each grid point.
- (Almost) **no extra cost for TABC in CEIMC** since we sum over twist angles to reduce the noise.

Finite size effects: TABC

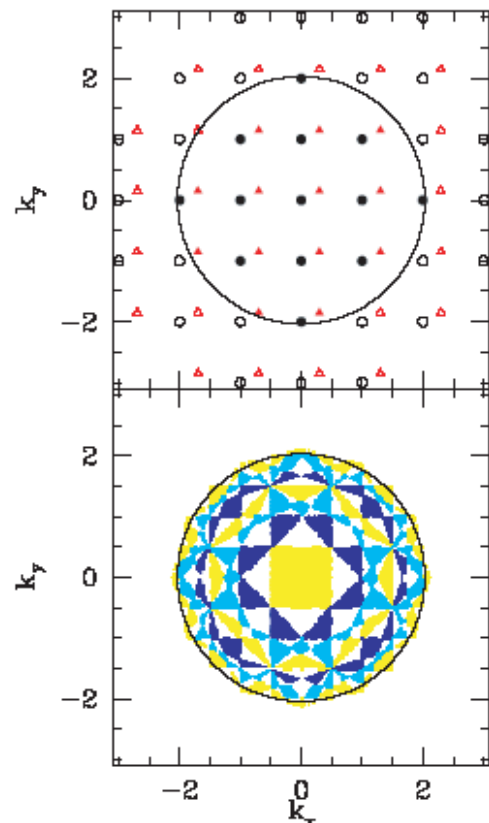


FIG. 1. Momentum distribution for 13 spinless fermions in a 2D square with side $L = 2\pi$. The top panel shows the occupied states (closed symbols) and empty states (open symbols) with zero twist (circles, PBC) and a twist equal to $2\pi(0.3, 0.15)$ (triangles). The circle shows the infinite system fermi surface. The bottom panel shows the occupied states with TABC. The colored regions show the occupied region for the lowest level (middle square), the third level, up to the outermost 13th level.

Lin, Zong, Ceperley PRE 64, 016702 (2001)

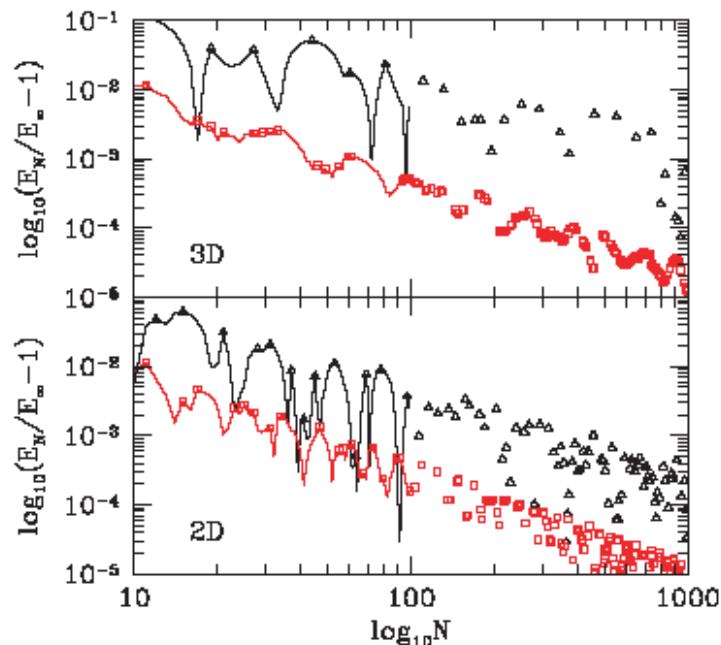


FIG. 2. Relative error of the energy versus number of particles with PBC (Δ) and TABC (\square) in 2D and 3D. The points shown are only those where the relative error has a local maximum. Curves are shown only for $N < 100$.

Sampling the electrons

VMC: in classical systems it is usually more efficient to move the particles one at a time by adding a random vector to a particle's coordinate. This remains true in VMC if we can update the Slater determinant efficiently (single row and column updates).

With **backflow** wave functions we would need to recompute the entire Slater determinant after any single particle move \implies **global moves**.

Sampling the electrons

VMC: in classical systems it is usually more efficient to move the particles one at a time by adding a random vector to a particle's coordinate. This remains true in VMC if we can update the Slater determinant efficiently (single row and column updates).

With **backflow** wave functions we would need to recompute the entire Slater determinant after any single particle move \implies **global moves**.

RQMC: at each move one end of the *many-body polymer* is randomly chosen. A number of links are cut at the sampled end and added to the opposite end. Detailed balance is imposed by computing the probability of the reverse move.

Sampling the electrons

VMC: in classical systems it is usually more efficient to move the particles one at a time by adding a random vector to a particle's coordinate. This remains true in VMC if we can update the Slater determinant efficiently (single row and column updates).

With **backflow** wave functions we would need to recompute the entire Slater determinant after any single particle move \implies **global moves**.

RQMC: at each move one end of the *many-body polymer* is randomly chosen.

A number of links are cut at the sampled end and added to the opposite end.

Detailed balance is imposed by computing the probability of the reverse move.

Problems: a) the **memory** of this algorithm in MC step scales as $(\#beads)^2/\text{acceptance}$.

b) **persistent configurations** can appear

Sampling the electrons

VMC: in classical systems it is usually more efficient to move the particles one at a time by adding a random vector to a particle's coordinate. This remains true in VMC if we can update the Slater determinant efficiently (single row and column updates).

With **backflow** wave functions we would need to recompute the entire Slater determinant after any single particle move \implies **global moves**.

RQMC: at each move one end of the *many-body polymer* is randomly chosen.

A number of links are cut at the sampled end and added to the opposite end.

Detailed balance is imposed by computing the probability of the reverse move.

Problems: a) the **memory** of this algorithm in MC step scales as $(\#beads)^2/\text{acceptance}$.

b) **persistent configurations** can appear

Bounce algorithm: we propose to choose at random one end of the chain at the beginning of the calculation and to reverse the growth direction upon rejection only.

It is possible to prove that it samples the correct probability distribution (Pierleoni Ceperley, ChemPhysChem 2005).

Nice scaling of the memory.

No persistent configurations observed.

The bounce algorithm

Bounce algorithm: choose at random one end of the chain at the beginning of the Markov chain and reverse the growth direction upon rejection only. Minimal modification of the algorithm and solve both problems

Proof of the Bounce algorithm:

- enlarge the configurational space $\{Q, d\}$ and define $P(Q, d \rightarrow Q', d')$.
- assuming ergodicity, the Markov chain converges to a unique stationary state, $\Upsilon(Q, d)$ solution of the eigenvalue equation:

$$\sum_{Q, d} \Upsilon(Q, d) P(Q, d \rightarrow Q', d') = \Upsilon(Q', d').$$

- allowed transitions

$$P(Q, d \rightarrow Q', d') \neq 0 \iff \begin{cases} d = d' & , Q \neq Q' & \text{accepted move} \\ d' = -d & , Q = Q' & \text{rejected move.} \end{cases}$$

- assume $d' = +1$. Since $\Pi(Q)$ does not depend on d

$$\Pi(Q')P(Q', -1 \rightarrow Q', 1) + \sum_{Q \neq Q'} \Pi(Q)P(Q, 1 \rightarrow Q', 1) = \Pi(Q').$$

The bounce algorithm

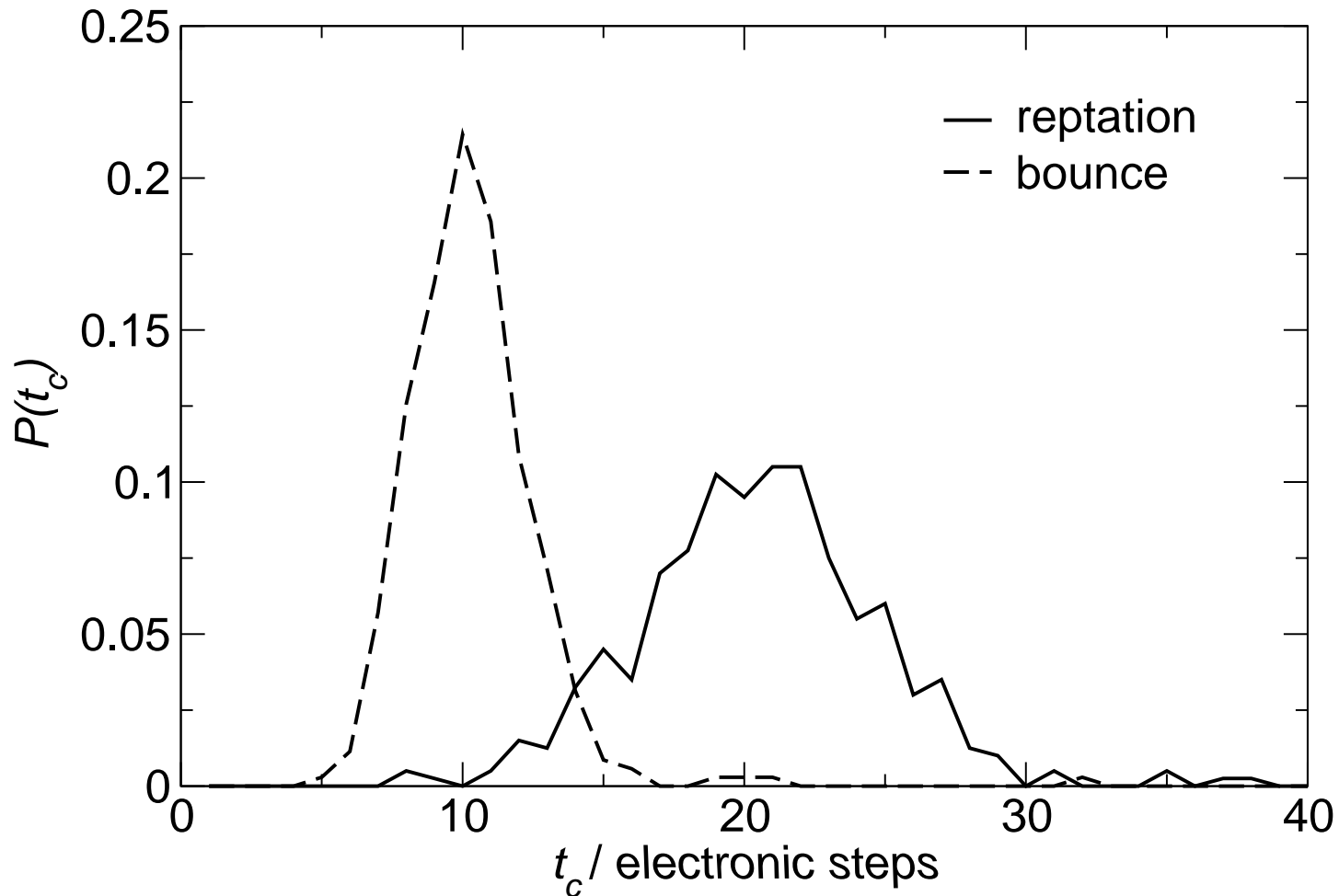
- **DB** ($\Pi(Q)P(Q, 1 \rightarrow Q', 1) = \Pi(Q')P(Q', -1 \rightarrow Q, -1)$) provides

$$\Pi(Q') \left[P(Q', -1 \rightarrow Q', 1) + \sum_Q P(Q', -1 \rightarrow Q, -1) \right] = \Pi(Q')$$

The term in the bracket exhausts all possibilities for a move from the state $(Q', -1)$, thus it adds to one. Hence $\Pi(Q)$ is a solution and by the theory of Markov chains, it is the unique probability distribution of the stationary state.

The bounce algorithm

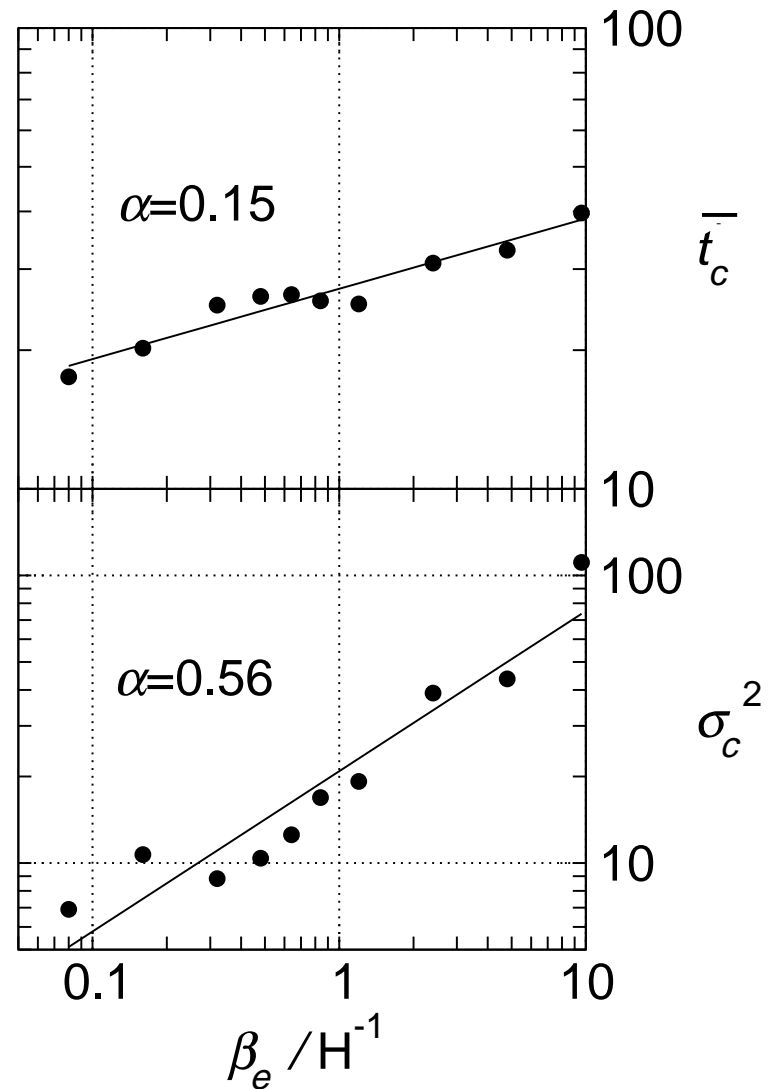
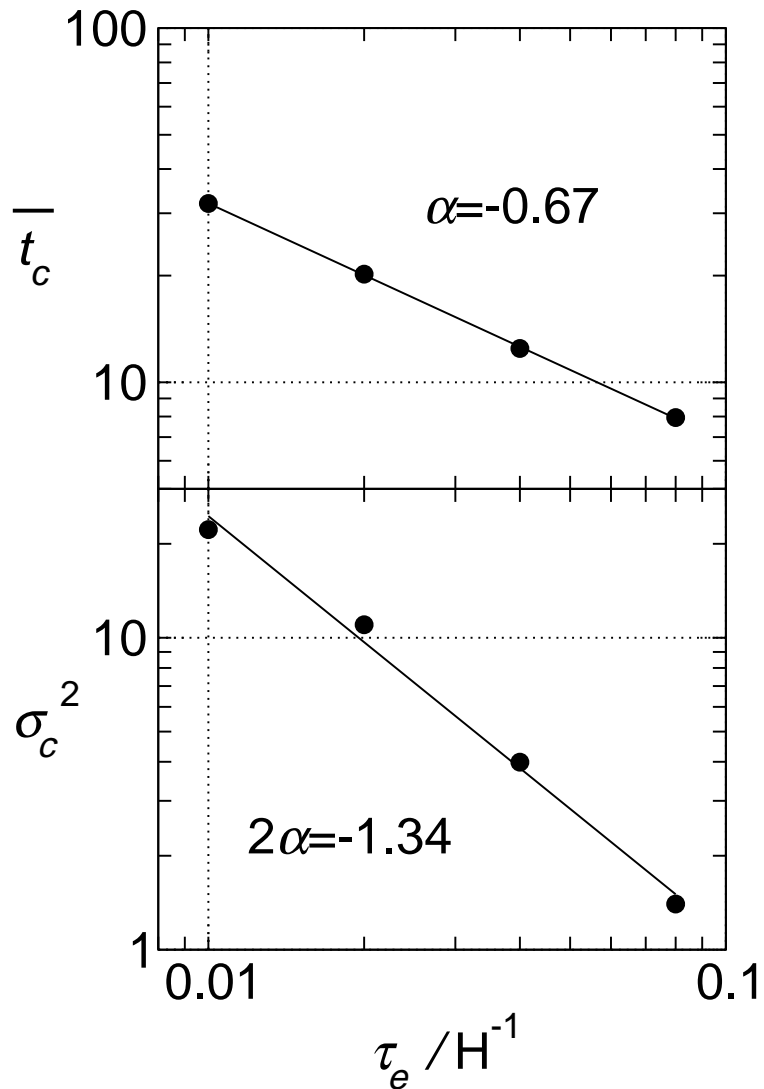
$$r_s=1.31, N_p=N_e=16, \tau_e=0.04, M=4$$



Probability distribution of the correlation time of the energy difference between two fixed protonic configurations (S, S').

The bounce algorithm

$$r_s = 1.31, N_p = N_e = 16$$



Two level sampling

Since the electronic part is much more expensive than computing any classical effective potential, in CEIMC we can use **two level Metropolis sampling** to improve the efficiency. Suppose $V_{cl}(S)$ is a reasonable proton-proton potential. The equilibrium distribution can be written as:

$$P(S) \propto e^{-\beta[E_{BO}(S) - V_{cl}(S)]} e^{-\beta V_{cl}(S)} = P_2(S)P_1(S)$$

A trial move is proposed and accepted or rejected based on a classical potential

$$A_1 = \min \left[1, \frac{T(S \rightarrow S')}{T(S' \rightarrow S)} \exp(-\beta[V_{cl}(S') - V_{cl}(S)]) \right]$$

Two level sampling

Since the electronic part is much more expensive than computing any classical effective potential, in CEIMC we can use **two level Metropolis sampling** to improve the efficiency. Suppose $V_{cl}(S)$ is a reasonable proton-proton potential. The equilibrium distribution can be written as:

$$P(S) \propto e^{-\beta[E_{BO}(S) - V_{cl}(S)]} e^{-\beta V_{cl}(S)} = P_2(S) P_1(S)$$

A trial move is proposed and accepted or rejected based on a classical potential

$$A_1 = \min \left[1, \frac{T(S \rightarrow S')}{T(S' \rightarrow S)} \exp(-\beta[V_{cl}(S') - V_{cl}(S)]) \right]$$

If we accept at the first level, the QMC energy difference is computed and the move accepted with probability

$$A_2 = \min [1, \exp(-\beta\Delta E_{BO} - u_B) \exp(\beta[V_{cl}(S') - V_{cl}(S)])]$$

where u_B is the noise penalty.

Quantum protons

- By increasing pressure or decreasing temperature, ionic quantum effects start to become relevant. Those effects are important for hydrogen at high pressure.

Quantum protons

- By increasing pressure or decreasing temperature, ionic quantum effects start to become relevant. Those effects are important for hydrogen at high pressure.
- Static properties of quantum systems at finite temperature can be obtained with Path Integral Monte Carlo method (PIMC).

We need to consider the thermal density matrix rather than the classical Boltzmann distribution:

$$\rho_P(S, S' | \beta) = \langle S | e^{-\beta(K_p + E_{BO})} | S' \rangle$$

The same formalism as in RQMC applies. However

1 - β is the **physical inverse temperature** now.

2 - to compute averages of diagonal operators we map quantum protons over ring polymers

3 - we limit to distinguishable particle so far ($T > T_d$), but Bose or Fermi statistics could be considered.

Quantum protons

- By increasing pressure or decreasing temperature, ionic quantum effects start to become relevant. Those effects are important for hydrogen at high pressure.
- Static properties of quantum systems at finite temperature can be obtained with Path Integral Monte Carlo method (PIMC).

We need to consider the thermal density matrix rather than the classical Boltzmann distribution:

$$\rho_P(S, S' | \beta) = \langle S | e^{-\beta(K_p + E_{BO})} | S' \rangle$$

The same formalism as in RQMC applies. However

1 - β is the **physical inverse temperature** now.

2 - to compute averages of diagonal operators we map quantum protons over ring polymers

3 - we limit to distinguishable particle so far ($T > T_d$), but Bose or Fermi statistics could be considered.

- **Factorization** $\beta = P\tau_p$ and **Trotter break-up**

For efficiency introduce an effective proton-proton potential $\hat{H}_{eff} = \hat{K}_P + \hat{V}_{eff}$

$$\hat{\rho}_P(\tau_p) = e^{-\tau_p[\hat{H}_{eff} + (\hat{E}_{BO} - \hat{V}_{eff})]} \approx e^{-\tau_p \hat{H}_{eff}} e^{-\tau_p[\hat{E}_{BO} - \hat{V}_{eff}]}$$

Quantum protons - 2

- We compute numerically the matrix elements of the **effective pair density matrix** $\hat{\rho}_{eff}^{(2)}(\tau_p)$. The effective N-body density matrix is approximated by

$$\langle S | \hat{\rho}_{eff}^{(N)}(\tau_p) | S' \rangle \approx \prod_{ij} \langle s_i, s_j | \hat{\rho}_{eff}^{(2)}(\tau_p) | s_i, s_j \rangle + O(n^3)$$

- We add the remaining term of the original Hamiltonian ($E_{BO} - V_{eff}$) at the level of the primitive approximation.
- With this Trotter break-up we found convergence to the continuum limit ($\tau_p \rightarrow 0$) for $1/\tau_p \geq 3000K$ which allows to simulate **systems at room temperature with only $M \approx 10$ proton slices** (for metallic hydrogen at $r_s = 1$).

Quantum protons - 3

In CEIMC quantum protons are (almost) for free !

- Suppose we run classical ions with a given level of noise $(\beta\sigma_{cl})^2$. Consider now representing the ions by P time slices. To have a comparable extra-rejection due to the noise we need a noise level per slice given by: $(\tau_p\sigma_k)^2 \approx (\beta\sigma_{cl})^2/P$ which provides $\sigma_k^2 \approx P\sigma_{cl}^2$. We can allow a noise per time slice P times larger which means considering P times less independent estimates of the energy difference per slice. However we need to run P different calculations, one for each different time slice, so that the amount of computing for a fixed global noise level is the same as for classical ions.

Quantum protons - 3

In CEIMC quantum protons are (almost) for free !

- Suppose we run classical ions with a given level of noise $(\beta\sigma_{cl})^2$. Consider now representing the ions by P time slices. To have a comparable extra-rejection due to the noise we need a noise level per slice given by: $(\tau_p\sigma_k)^2 \approx (\beta\sigma_{cl})^2/P$ which provides $\sigma_k^2 \approx P\sigma_{cl}^2$. We can allow a noise per time slice P times larger which means considering P times less independent estimates of the energy difference per slice. However we need to run P different calculations, one for each different time slice, so that the amount of computing for a fixed global noise level is the same as for classical ions.
- When using TABC, for any proton time slice we should in principle perform a separate evaluation of the BO energy difference averaging over all twist angles. We have checked that, at each proton step, we can randomly assign a subset of twists at each time slice and get the same results.

Quantum protons - 3

In CEIMC quantum protons are (almost) for free !

- Suppose we run classical ions with a given level of noise $(\beta\sigma_{cl})^2$. Consider now representing the ions by P time slices. To have a comparable extra-rejection due to the noise we need a noise level per slice given by: $(\tau_p\sigma_k)^2 \approx (\beta\sigma_{cl})^2/P$ which provides $\sigma_k^2 \approx P\sigma_{cl}^2$. We can allow a noise per time slice P times larger which means considering P times less independent estimates of the energy difference per slice. However we need to run P different calculations, one for each different time slice, so that the amount of computing for a fixed global noise level is the same as for classical ions.
- When using TABC, for any proton time slice we should in principle perform a separate evaluation of the BO energy difference averaging over all twist angles. We have checked that, at each proton step, we can randomly assign a subset of twists at each time slice and get the same results.
- We need to move all slices of all protons together. This limits the length of proton paths, therefore the temperature we can achieve. **It is essential to use the best possible Trotter factorization!!**

Summary of CEIMC method

- Given an initial configuration of the electronic path $Q = \{R_1, \dots, R_t\}$ and the protonic path $P = \{S_1, \dots, S_P\}$, propose a trial protonic move P' with a suitable transition probability (depending on the particular system).

Summary of CEIMC method

- Given an initial configuration of the electronic path $Q = \{R_1, \dots, R_t\}$ and the protonic path $P = \{S_1, \dots, S_P\}$, propose a trial protonic move P' with a suitable transition probability (depending on the particular system).
- Assign at random an equal number of twist angles to any proton slice and run many independent electronic calculations for each twist angle: **ideal for parallel computers !**

Summary of CEIMC method

- Given an initial configuration of the electronic path $Q = \{R_1, \dots, R_t\}$ and the protonic path $P = \{S_1, \dots, S_P\}$, propose a trial protonic move P' with a suitable transition probability (depending on the particular system).
- Assign at random an equal number of twist angles to any proton slice and run many independent electronic calculations for each twist angle: **ideal for parallel computers !**
- Sample the electronic configuration space with the importance sampling distribution depending on both P and P' .

Summary of CEIMC method

- Given an initial configuration of the electronic path $Q = \{R_1, \dots, R_t\}$ and the protonic path $P = \{S_1, \dots, S_P\}$, propose a trial protonic move P' with a suitable transition probability (depending on the particular system).
- Assign at random an equal number of twist angles to any proton slice and run many independent electronic calculations for each twist angle: **ideal for parallel computers !**
- Sample the electronic configuration space with the importance sampling distribution depending on both P and P' .
- Use reweighting to compute energy difference Δ and variance σ^2 by averaging results over all twist angles and proton slices

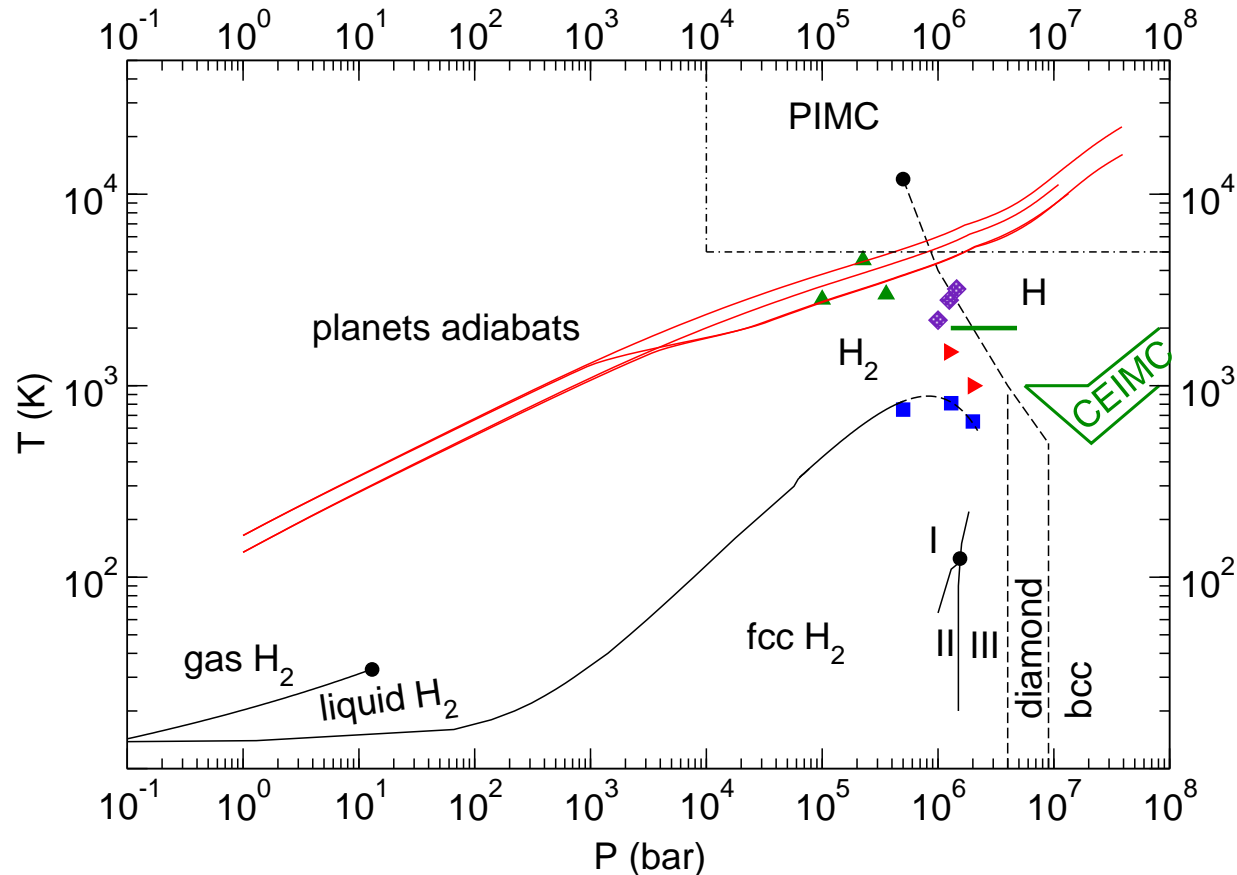
Summary of CEIMC method

- Given an initial configuration of the electronic path $Q = \{R_1, \dots, R_t\}$ and the protonic path $P = \{S_1, \dots, S_P\}$, propose a trial protonic move P' with a suitable transition probability (depending on the particular system).
- Assign at random an equal number of twist angles to any proton slice and run many independent electronic calculations for each twist angle: **ideal for parallel computers !**
- Sample the electronic configuration space with the importance sampling distribution depending on both P and P' .
- Use reweighting to compute energy difference Δ and variance σ^2 by averaging results over all twist angles and proton slices
- Performe the Metropolis test with the penalty method

Summary of CEIMC method

- Given an initial configuration of the electronic path $Q = \{R_1, \dots, R_t\}$ and the protonic path $P = \{S_1, \dots, S_P\}$, propose a trial protonic move P' with a suitable transition probability (depending on the particular system).
- Assign at random an equal number of twist angles to any proton slice and run many independent electronic calculations for each twist angle: **ideal for parallel computers !**
- Sample the electronic configuration space with the importance sampling distribution depending on both P and P' .
- Use reweighting to compute energy difference Δ and variance σ^2 by averaging results over all twist angles and proton slices
- Performe the Metropolis test with the penalty method
- Compute average quantities for the old protonic configuration P using reweighting.

Hydrogen: phase diagram



Continuous transition lines (in black): experimental results

dashed lines: theoretical prediction from various methods

red lines: model adiabats for the interior of the giant planets of the solar system

diamonds: shock-waves experiments through liquid metalization (Weir et al. PRB '96)

squares: CPMD predictions of molecular melting (Bonev et al, Nature '04)

right-triangle: CPMD predictions for molecular dissociation in the liquid phase (Scandolo, PNAS '03).

in green: CEIMC predictions

Trial wave functions: hystorical record

- 2001/02: [Ceperley, Dewing, Pierleoni: Lecture Notes in Physics, vol 605, (2002)]
S(pw)-J(rpa)+EXTRA+SELF+3BODY+ep-BF+ee-BF: 12 variational parameters

$$\Psi_T(\vec{R}|S) = \det(e^{i\vec{k}_i \cdot \vec{x}_j}) \exp \left(- \sum_{i=1}^{N_e} \left[\frac{1}{2} \sum_{j \neq i}^{N_e} \tilde{u}_{ee}(r_{ij}) - \sum_{j=1}^{N_p} \tilde{u}_{ep}(r_{ij}) - \frac{1}{2} \vec{G}(i) \cdot \vec{G}(i) \right] \right)$$

backflow:

$$\vec{x}_i = \vec{r}_i + \sum_{j \neq i}^{N_e} \eta_{ee}(r_{ij})(\vec{r}_i - \vec{r}_j) + \sum_{j=1}^{N_p} \eta_{ep}(r_{ij})(\vec{r}_i - \vec{r}_j)$$

$$\eta_\alpha(r) = \lambda_b^\alpha \exp[-(r/w_b^\alpha)^2]$$

3body:

$$\mathbf{G}(i) = \sum_{j \neq i}^{N_e} \xi_{ee}(r_{ij})(\vec{r}_i - \vec{r}_j) + \sum_{j=1}^{N_p} \xi_{ep}(r_{ij})(\vec{r}_i - \vec{r}_j)$$

$$\tilde{u}_{ee}(r) = u_{ee}(r) - \xi_{ee}^2(r)r^2$$

$$\tilde{u}_{ep}(r) = u_{ep}(r) - \xi_{ep}^2(r)r^2$$

$$\xi(r) = \lambda_T^\alpha \exp[-(r/w_T^\alpha)^2]$$

Trial wave functions: hystorical record

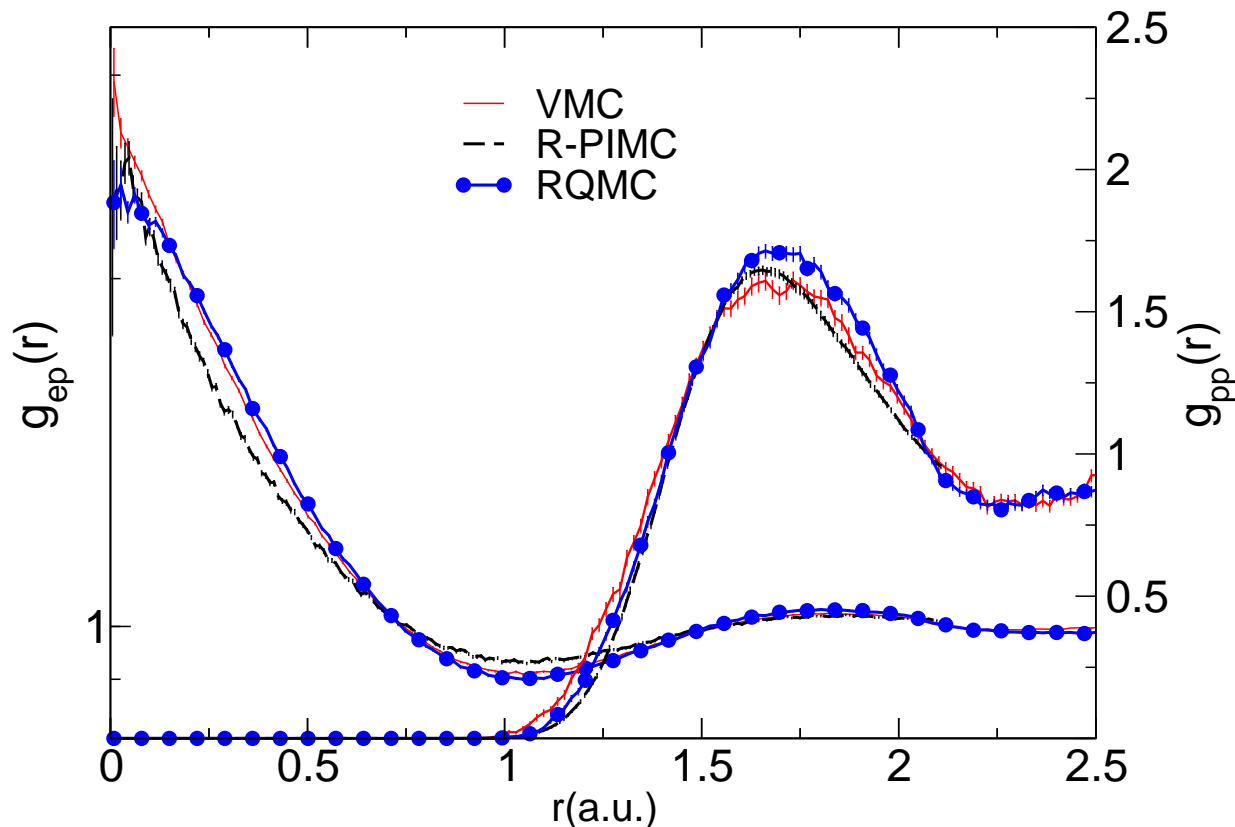
- 2003/04: [Holzmann, Ceperley, Pierleoni, Esler PRE 68, 046707 (2003)]
Analytical expressions for the 3body and BF functions: **PARAMETER FREE TRIAL FUNCTION**.

It performs very well, compared to the numerically optimized version, both for protons in crystal structures and in disordered configurations.

N_p		E_{VMC} (h/at)	σ^2	E_{DMC}
16	LDA	-0.4870(10)		-0.4890(5)
	BF3-O ep	-0.4857(1)	0.0317 (5)	-0.4900 (1)
	BF-A	-0.4850(1)	0.0232(1)	-0.4905(1)
54	LDA	-0.5365(5)		-0.5390(5)
	BF3-O ep	-0.5331 (6)	0.033 (1)	-0.5381 (1)
	BF-A	-0.5323(1)	0.0222(2)	-0.5382(1)
128	LDA	-0.4962(2)		-0.4978(2)
	BF3-O ep	-0.4934 (2)	0.035 (2)	-0.4958 (3)
	BF-A	-0.4928(2)	0.030(1)	-0.4978(4)

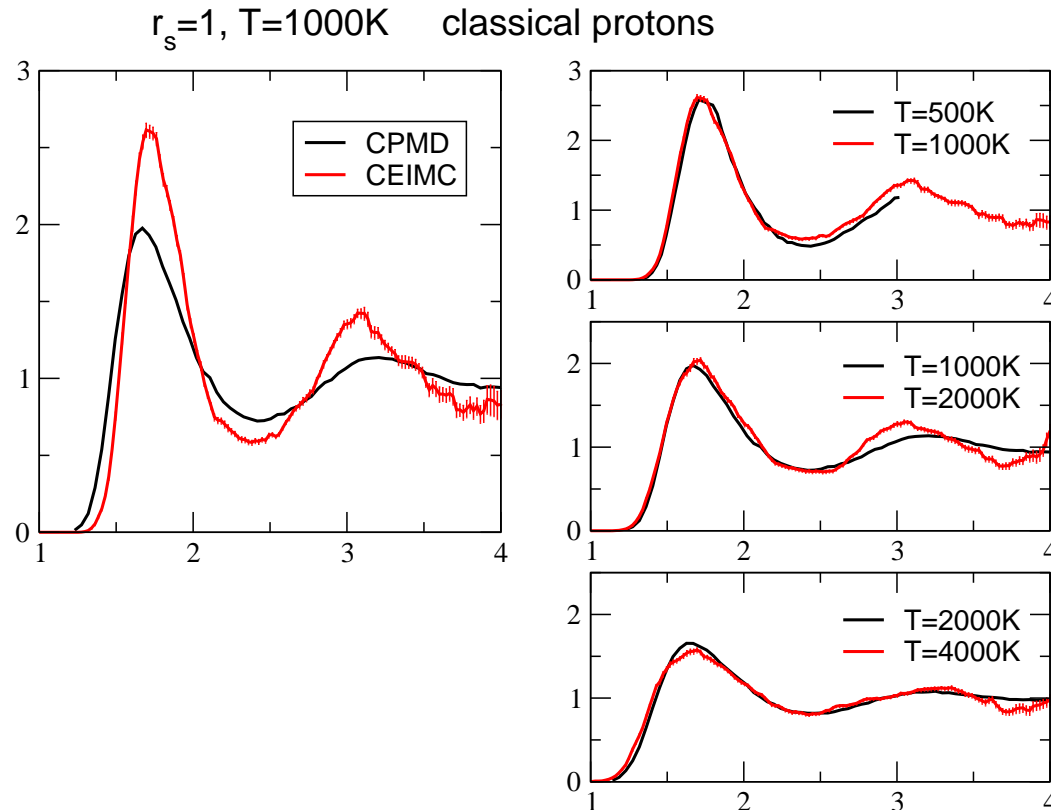
$r_s=1.31$, $T=0K$, BCC proton crystal, zero phase. (LDA=Natoli et al PRL 1993)

2003/04: analytical SJ3BF



CEIMC vs RPIMC for electron-proton and proton-proton correlation function at $r_s = 1, T = 5000K, N_p = N_e = 16, \Gamma$ point. RPIMC has ground state free particle nodes.

2003/04: analytical SJ3BF



● CPMD-LDA predicts less structure than observed in CEIMC.

● Proton melting:

- $T_m(LDA) \simeq 350K$ (Lindemann ratio) (Kohanoff Hansen '95)

- $1000K \leq T_m(CEIMC) < 1500K$ (dynamical criterium)

Trial wave functions: hystorical record

- 2005/06: [Delaney, Pierleoni, Ceperley, PRL 2006]
Band structure and self consistent (LDA) orbital+RPA-Jastrow (cusp corrected) to approach lower densities (molecular dissociation region).
No extra variational parameters to optimize at the QMC level.
At $r_s \leq 1.3$ they provide lower energy than the metallic wave function.
Used to study the molecular dissociation process in the liquid.

Nodal surfaces accuracy

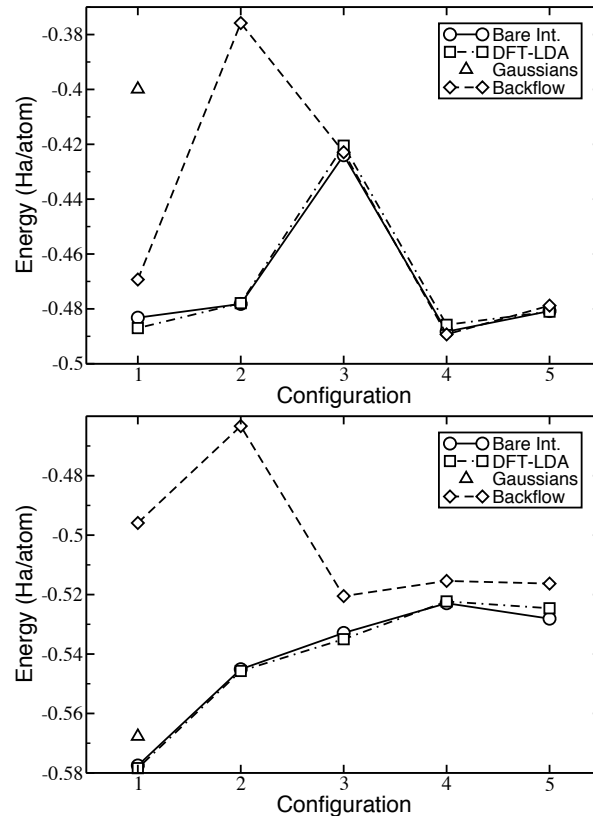
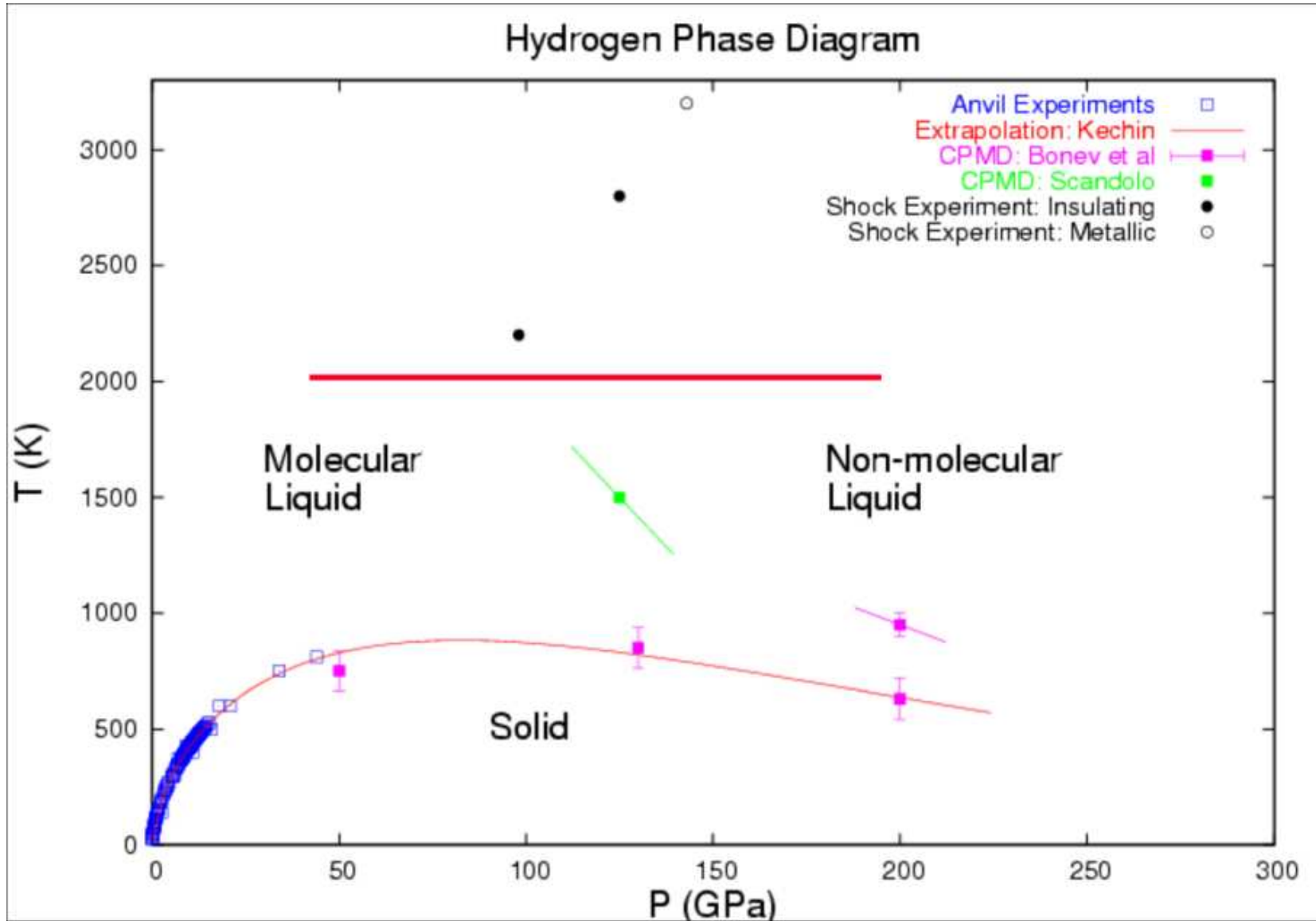
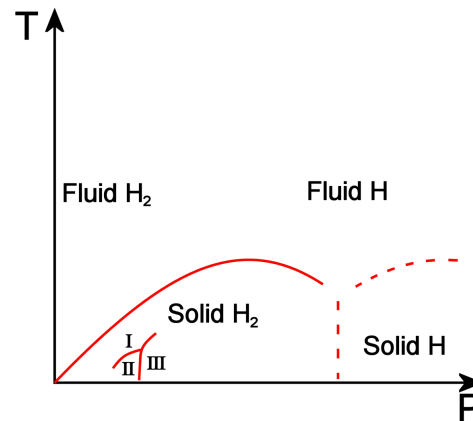
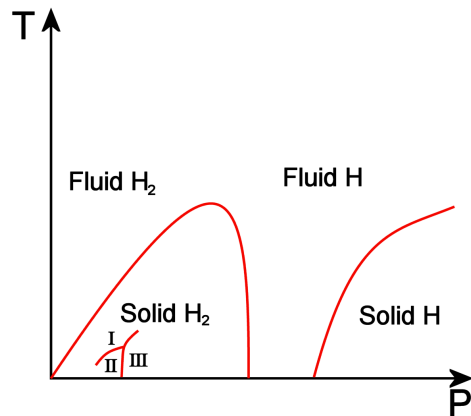
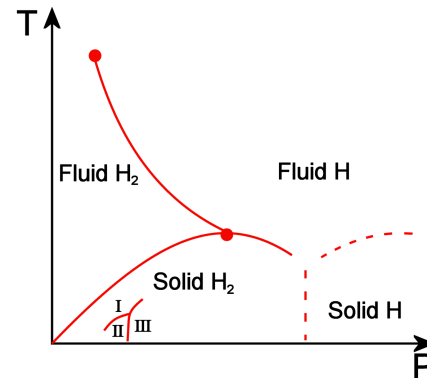
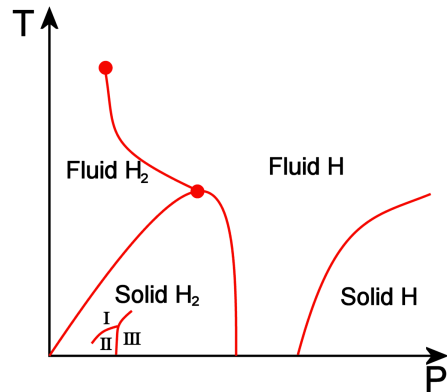


FIG. 1: RQMC total energy for five different crystal configurations at two different densities (upper graph $V = 9.42$ a.u./atom or $r_s = 1.31$; lower $V = 33.51$ a.u./atom or $r_s = 2.0$) using a number of different Slater-Jastrow wavefunctions. Configuration 1 is molecular, 2–5 are non-molecular. Owing to the variational principle, a lower energy implies a better wavefunction. DFT-LDA and bare electron-proton bands (see text) provide the best and most transferable orbitals for the Slater determinant. Gaussian for configuration 1 refers to localized molecular orbitals.

Liquid-Liquid PT (PPT)





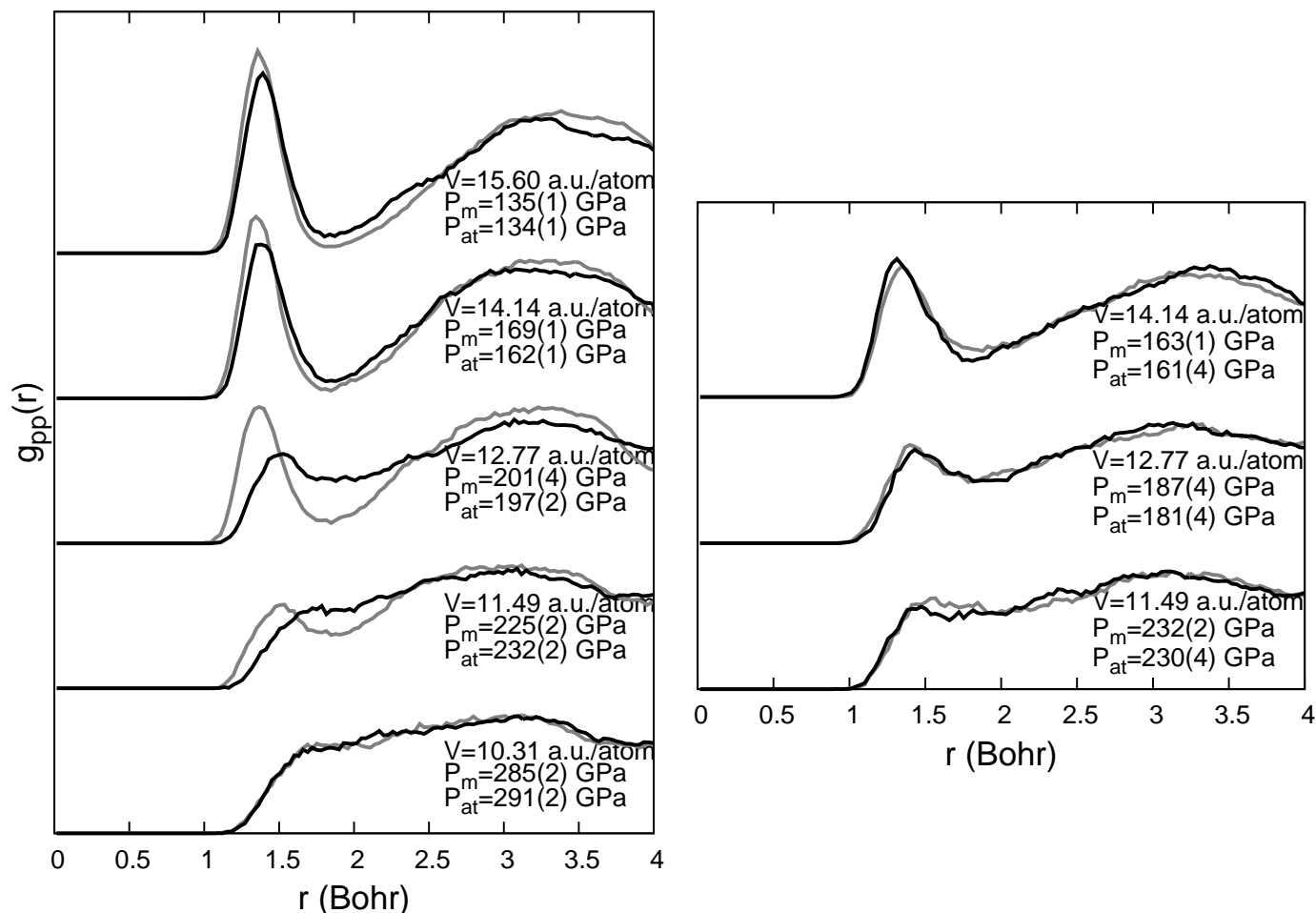
- below a critical temperature, CPMD predicts the existence of a discontinuous molecular dissociation transition with pressure also coinciding with the MIT.
- the reentrant melting of the molecular system, observed with CPMD, and the large ZPM of the protons at low temperature could suggest the presence of a low temperature fluid region between the molecular and the atomic solid.

Liquid-Liquid PT: CEIMC

- Simulation details:
 - 32 and 54 atoms, NVT ensemble
 - single electron orbitals from a band structure calculation with the bare coulomb potential.
 - self-consistent KS orbitals provide only marginally better energies than band-structure orbitals (on selected static proton configuration).
 - T=2000K, 1500K.
 - P=0.5-2 Mbars
 - 216 twist angles
 - classical protons so far

Delaney, Pierleoni, Ceperley: PRL **97**, 235702 (2006)

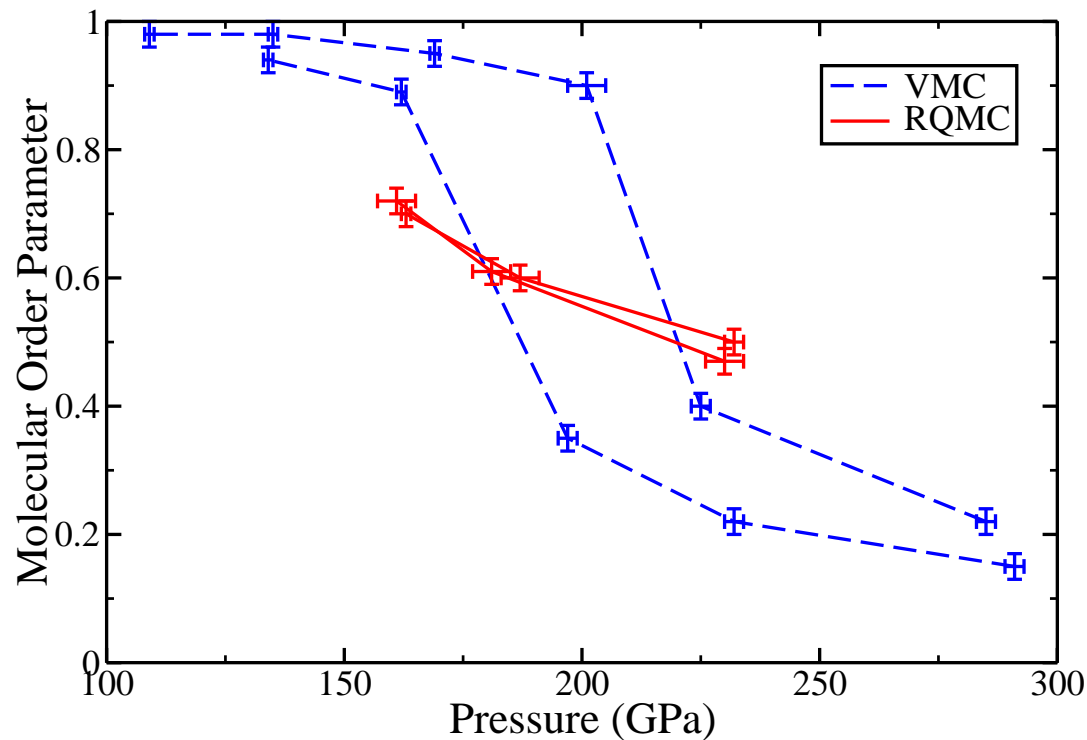
Liquid-Liquid PT: CEIMC



$N_p = 32, T = 2000K$, NVT ensemble. VMC (left pane), RQMC (right pane).

Grey lines from a molecular fluid and black from an atomic fluid.

Liquid-Liquid PT: CEIMC

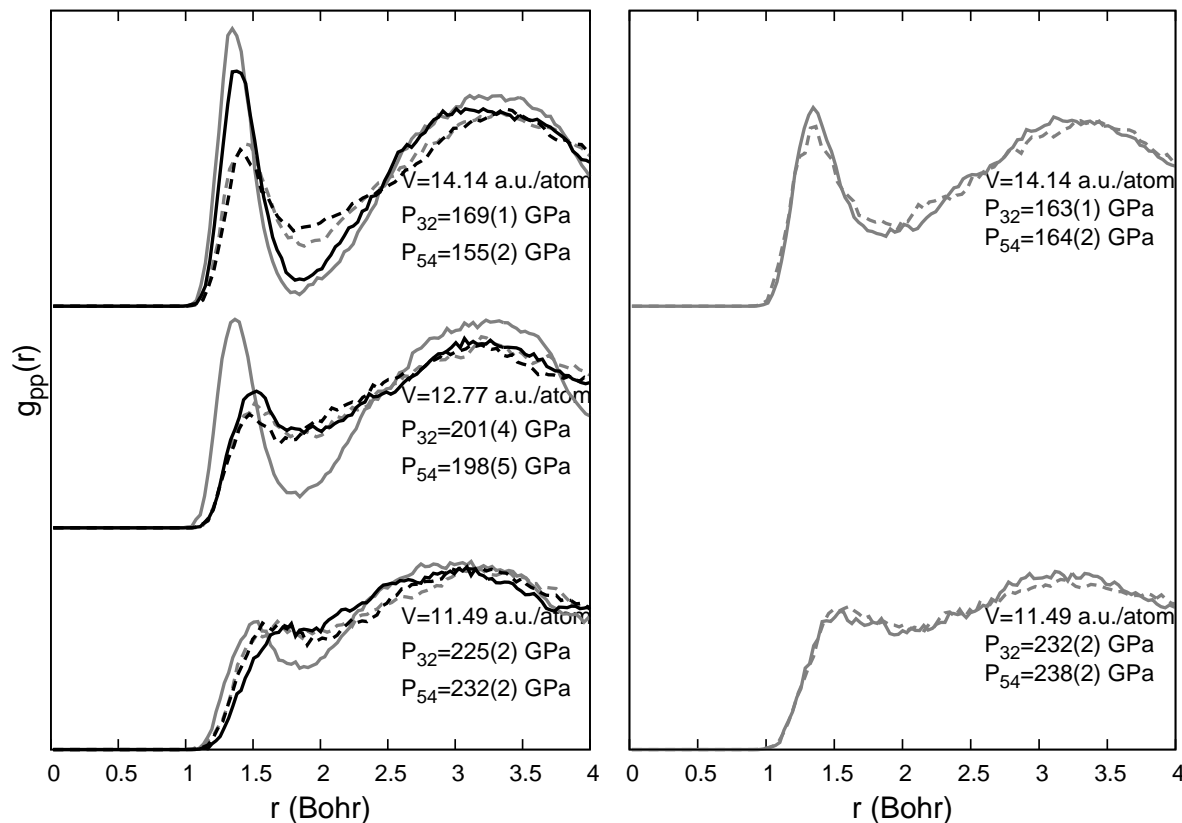


- Molecular order parameter: λ

$$g(r) = \lambda g_m(r; \{\alpha\}) + (1 - \lambda) g_{at}(r; \{\gamma\})$$

- **VMC**: hysteresis, indication of a 1st order transition
- **RQMC**: no hysteresis, continuous transition.

Liquid-Liquid PT: CEIMC



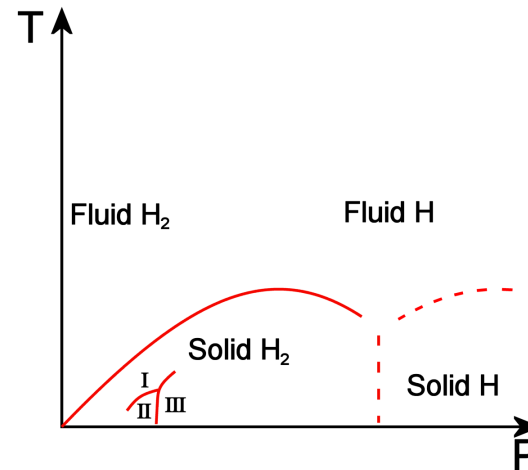
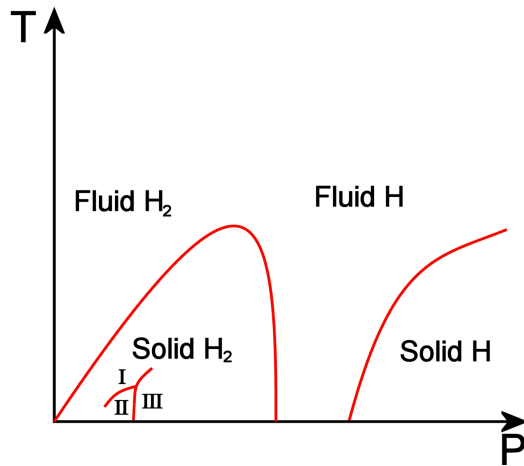
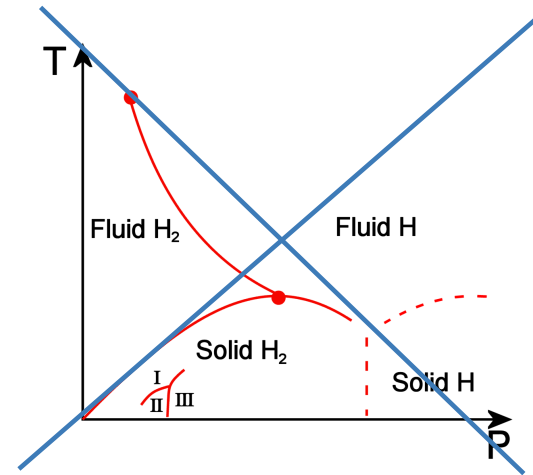
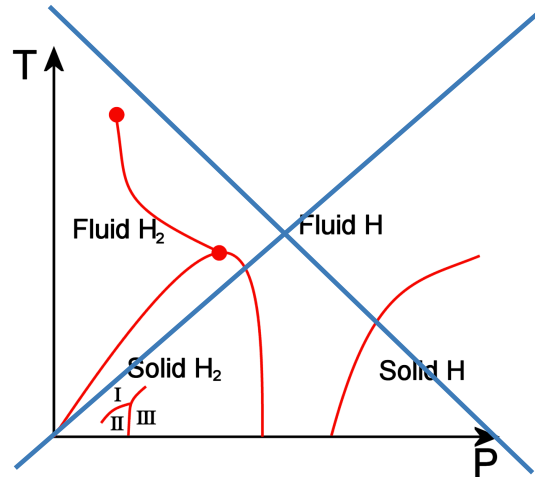
Solid lines are 32-atom simulations, dashed are 54 atoms. Grey lines are simulations started from a molecular fluid and black are from an atomic fluid.

- finite size effects are large with VMC supporting the presence of a discontinuous transition
- finite size effects are undetectable with RQMC supporting a continuous dissociation

Liquid-Liquid PT: CEIMC

- Main conclusions:
 - using VMC a clear hysteresis is observed
presence of metastable states \implies 1st order phase transition?
 - qualitative agreement with CPMD but at higher pressure (2Mbars vs 1.25Mbars).
 - using RQMC the hysteresis goes away \implies continuous molecular dissociation
 - Size effects check 54 atoms:
 - detectable size effects with VMC
 - undetectable with RQMC
 - same scenario is found at T=1500K.

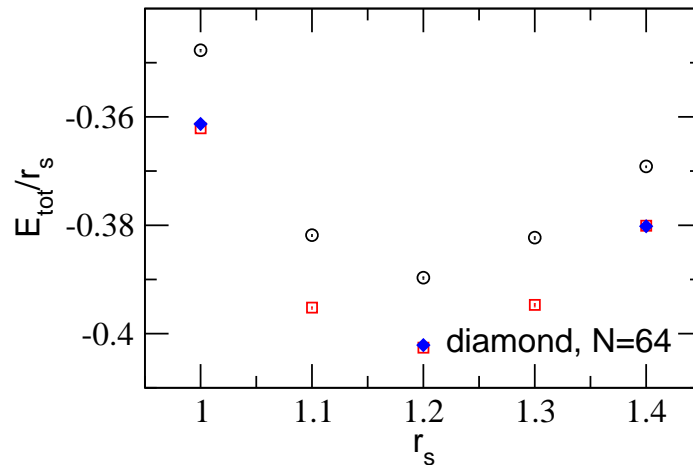
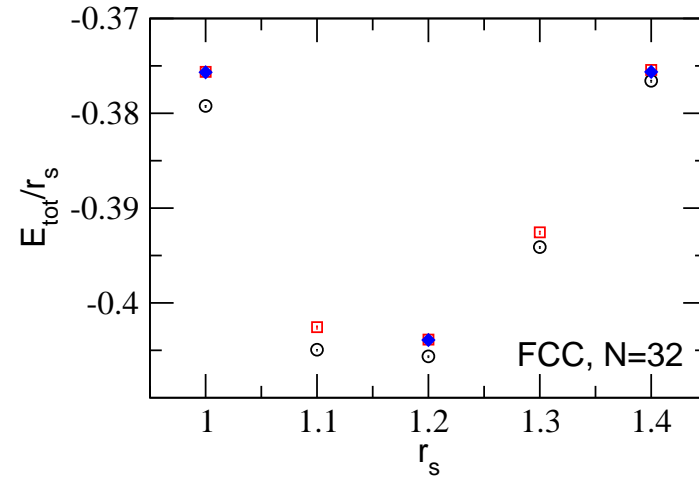
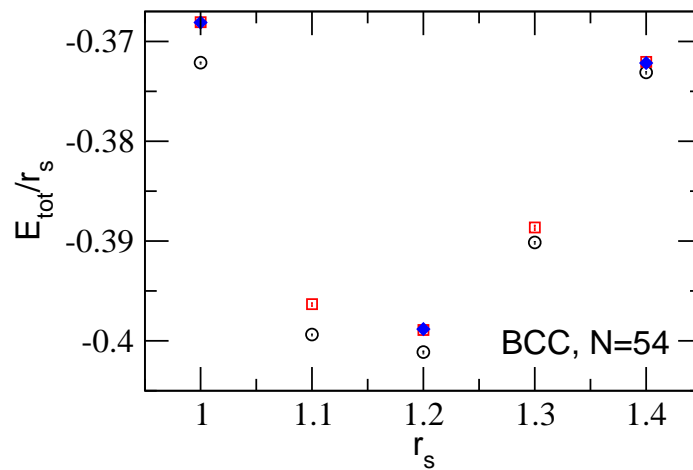
Proposed Scenarios



- CEIMC do not support the existence of a first order LLPT: upper panels are discarded
- GS-QMC (Ceperley 87) do not support the presence of a ground state liquid phase

Metallic hydrogen: crystal phases

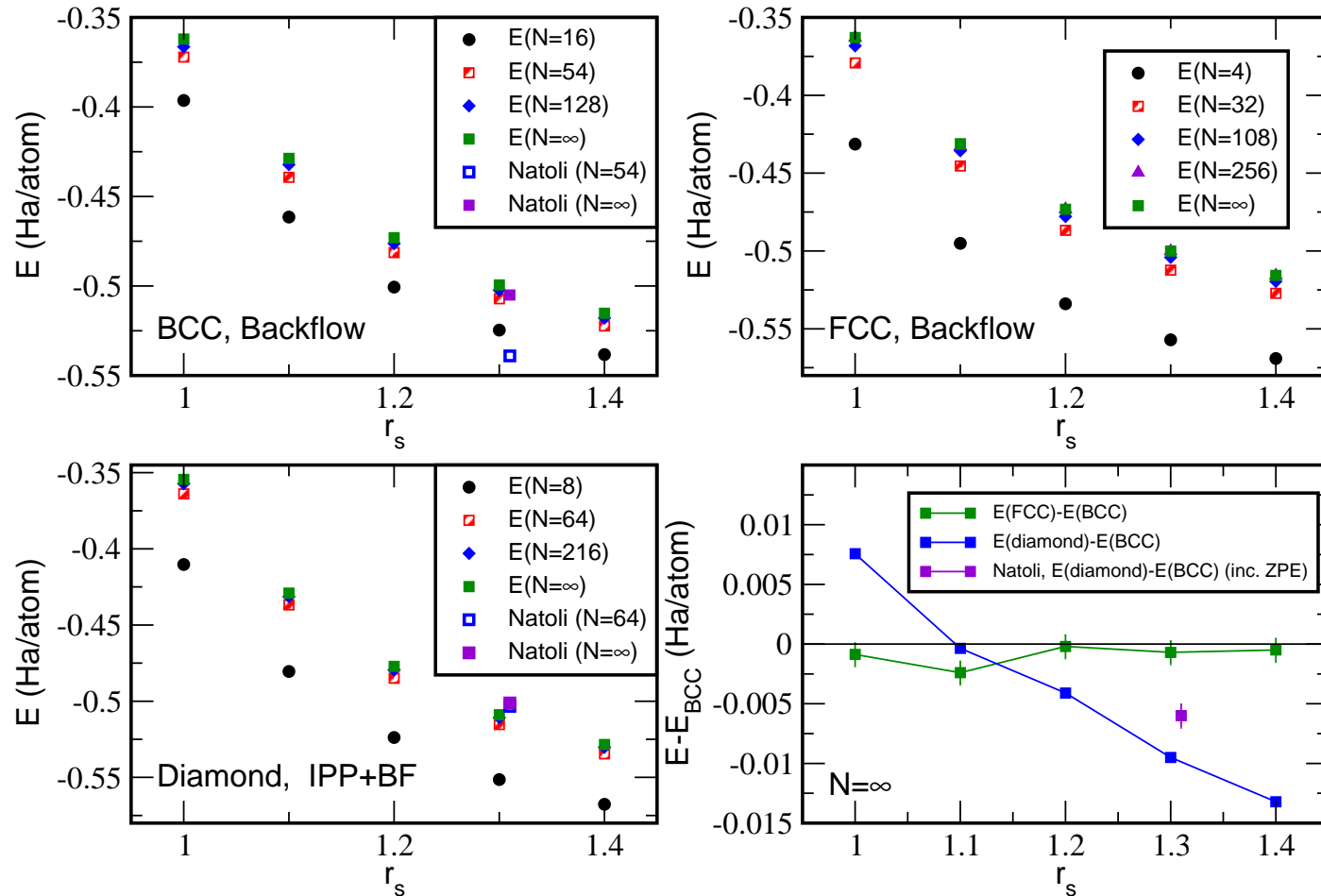
RQMC Wavefunction Tests
108 fixed twists, $\tau_e=0.005$, $\beta_e=0.475$



Metallic hydrogen: crystal phases 2

Hydrogen Ground-state Crystal Structure

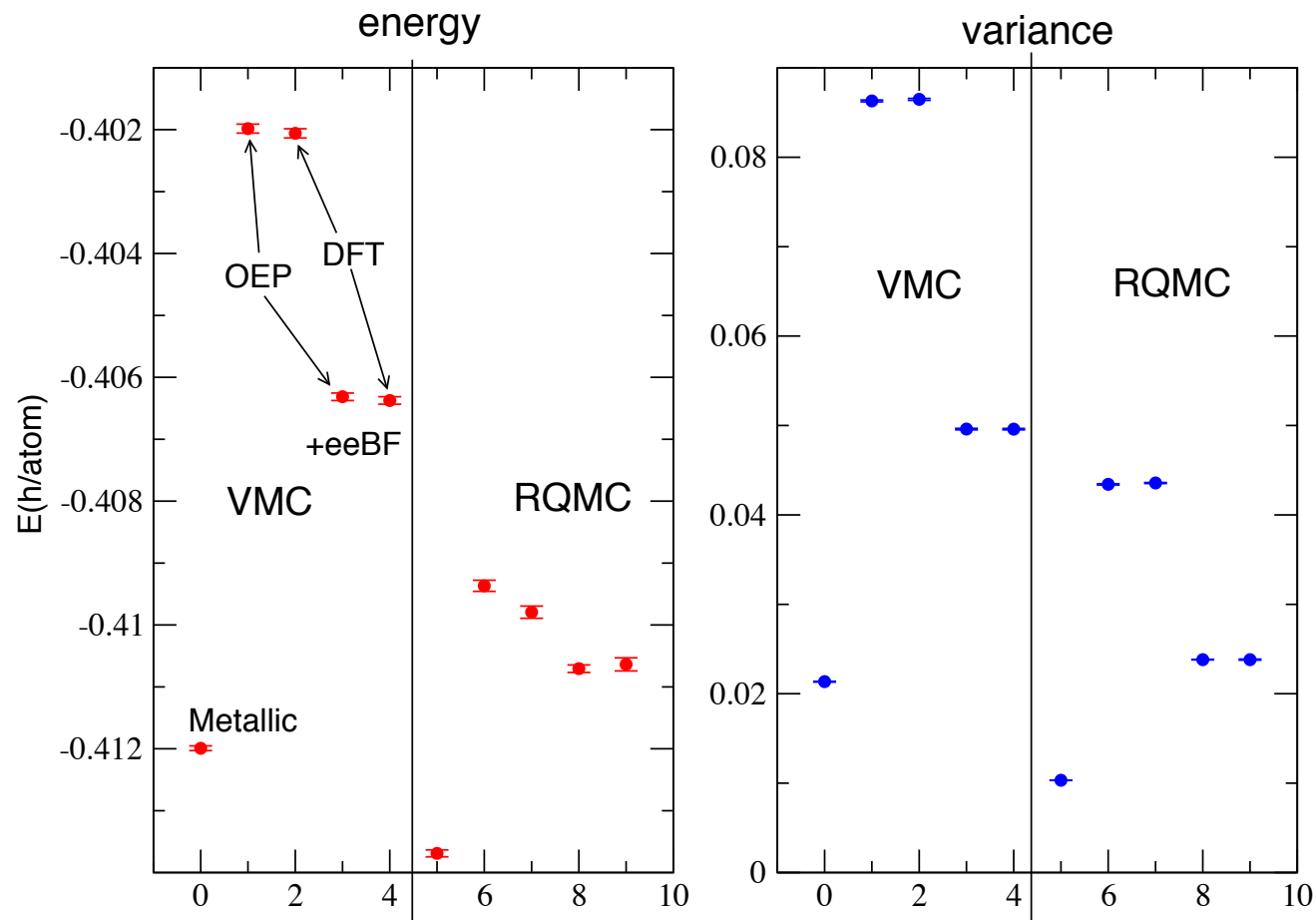
108 fixed twists, RQMC: $\tau_e=0.005$, $\beta_e=0.505$



Trial wave functions improvement

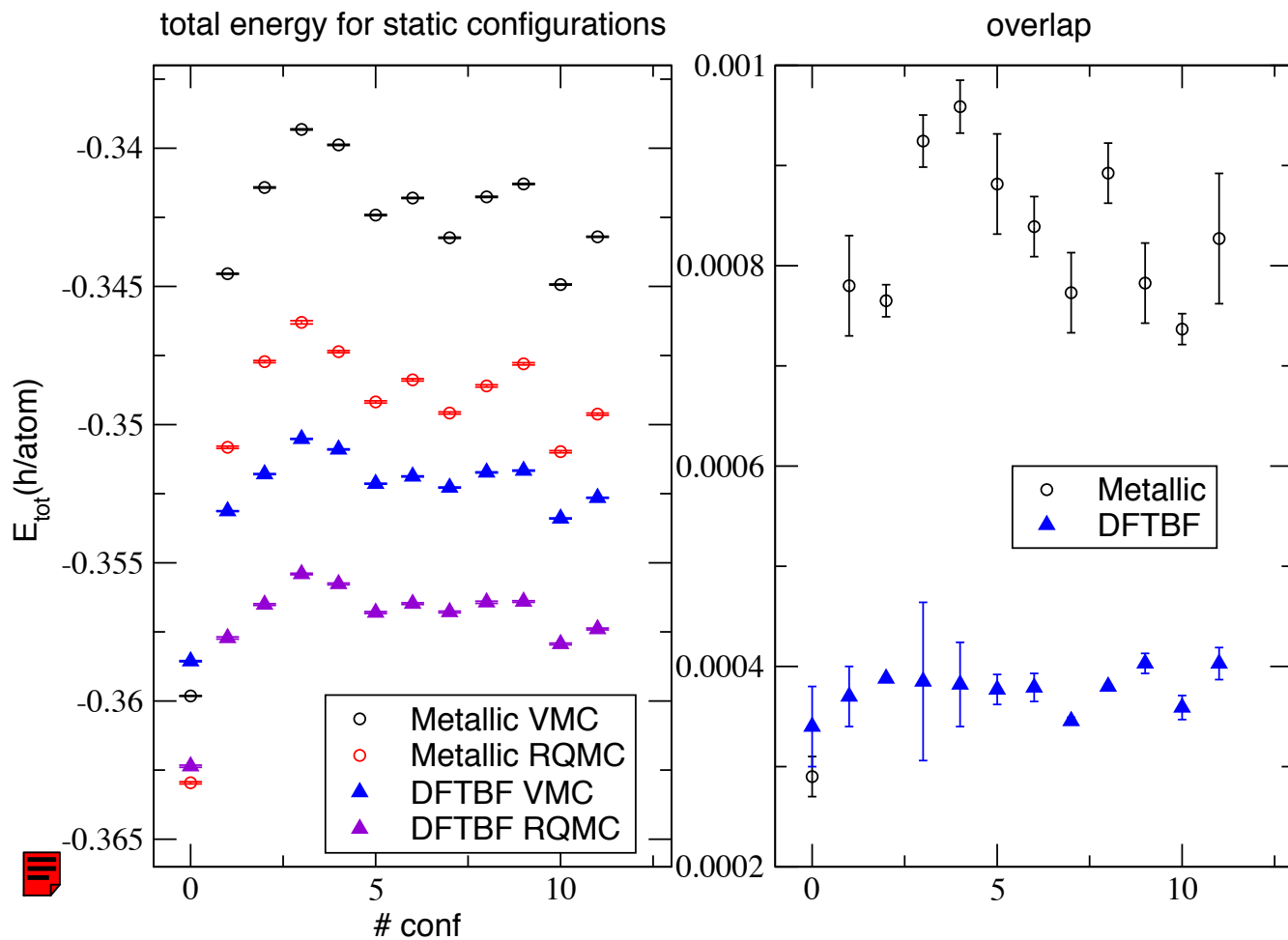
- 2007: DFT/band orbitals (cusp corrected) + J-RPA + eeBF-A.
eeBF improves the energy and reduces by a factor of two the variance !!!

Diamond lattice: $N_p=8$, $R_s=1$, 108 twists

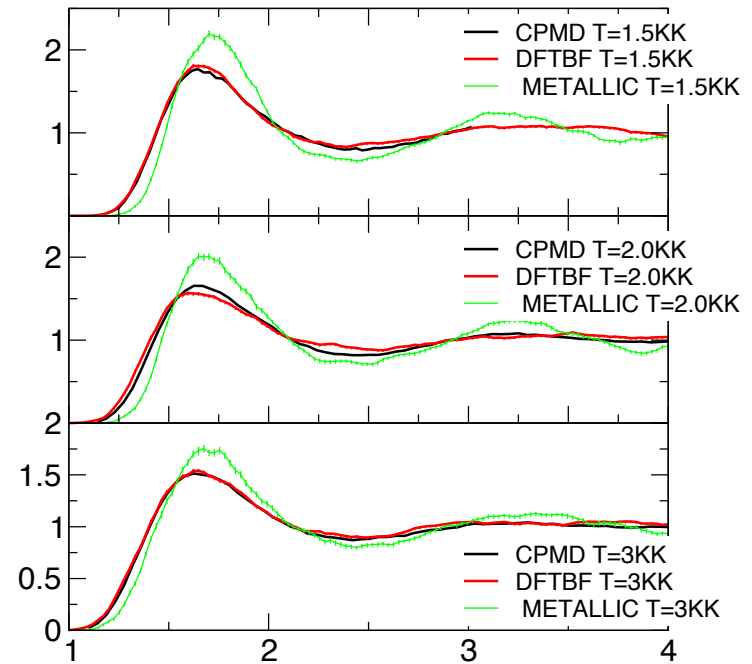
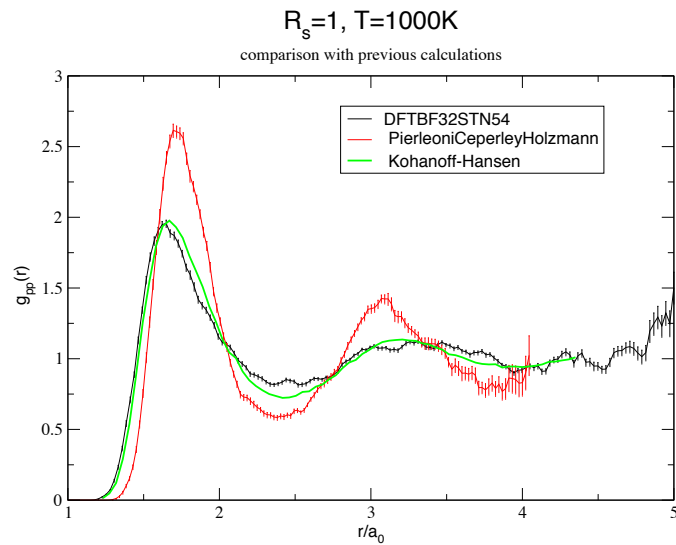


Test of the trial function: Metallic vs DFTBF

$R_s=1$, $N_p=54$: Metallic vs DFTBF trial functions



Metallic hydrogen: liquid phase

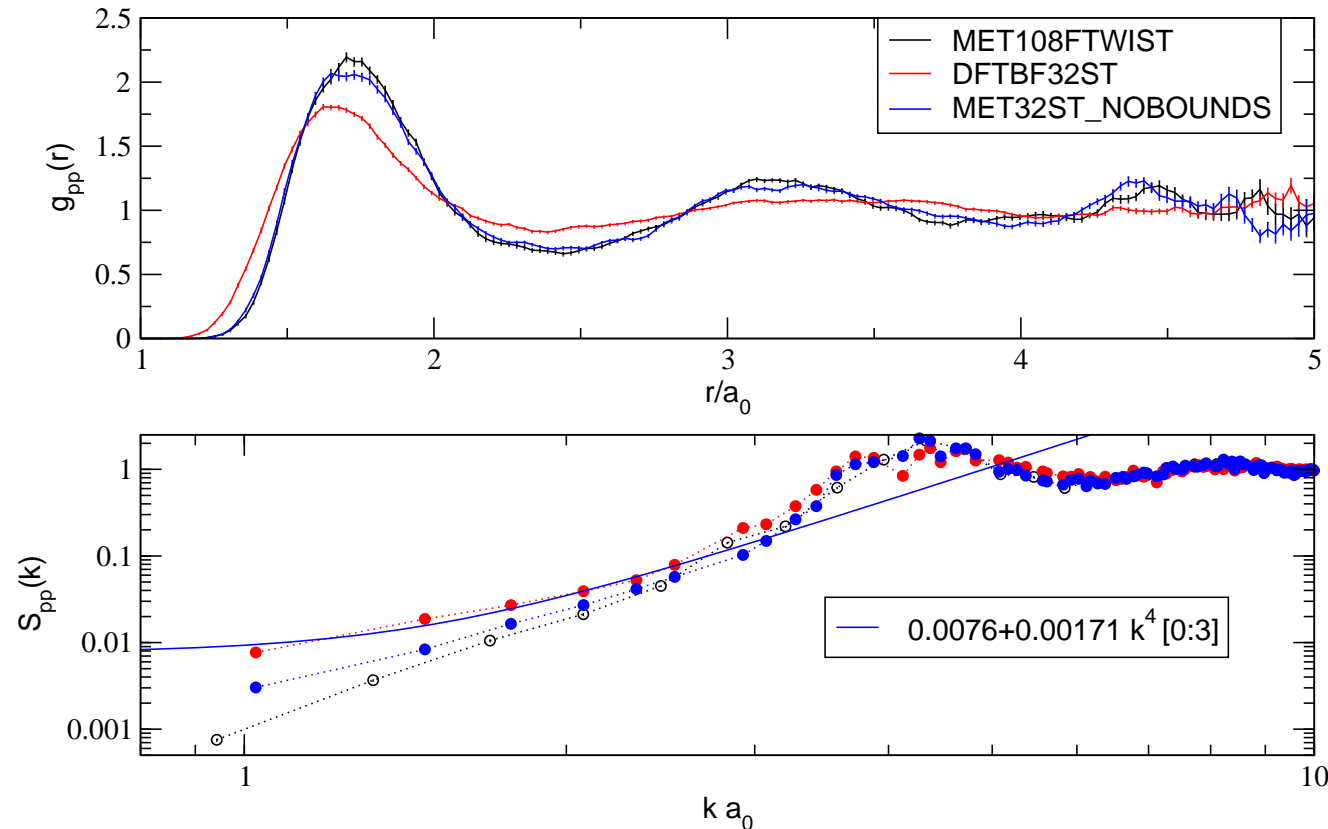


- DFTBF wf is in very good agreement with CPMD data but not with the SJ3BF (Metallic) wf.

Metallic hydrogen: liquid phase

$N_p=54$ classical protons: $R_s=1$, $T=1500\text{K}$

Metallic wf vs DFTBF, VMC-TABC



- Metallic wf does not seem to have the correct long wavelength behaviour and to provide the correct compressibility at $k=0$.

● In progress

- Quantitative location of the melting line in the metallic-atomic phase
- Study of the low temperature crystal structure and possible appearance of a stable low-temperature liquid.
- Equation of state along the planets adiabates.
- Demixing in H-He mixtures (high temperature).

● Method developments

- Constant-pressure algorithm to investigate structural phase transitions.
- Implementation of QMC forces for “dynamical simulations”.
- Use of pseudopotentials to extend the method to heavier elements:
WATER!!! (or other interesting systems).

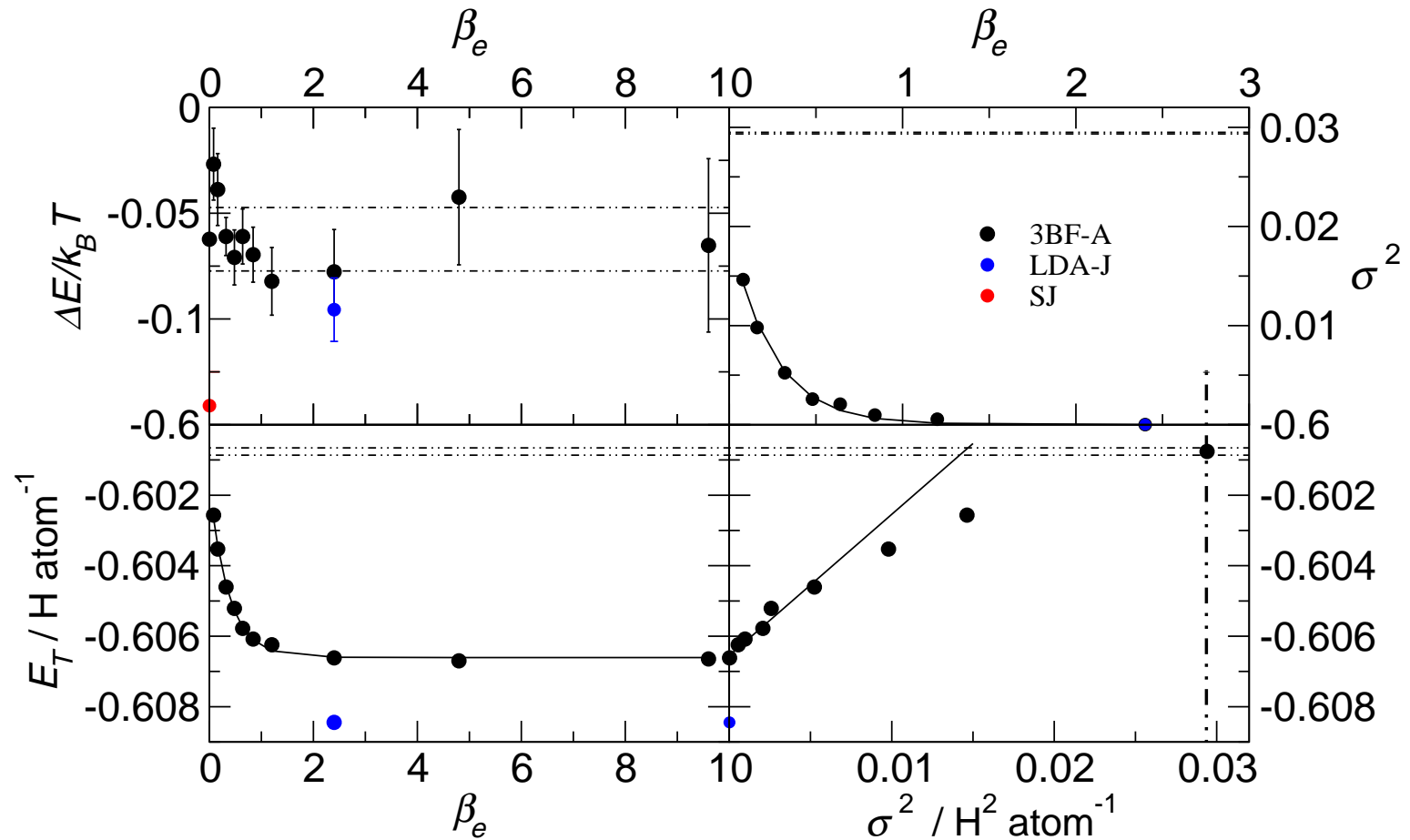
Related publications

1. D.M. Ceperley, M. Dewing and C. Pierleoni “The coupled Electronic-Ionic Monte Carlo simulation method”, *Lecture Notes in Physics*, vol 605, pp 473-499.
2. M. Holzmann., D.M.Ceperley, C. Pierleoni and K. Esler “Backflow correlation in the electron gas and metallic hydrogen” *Phys. Rev. E* **68**, 046707 (2003).
3. C. Pierleoni, D.M. Ceperley and M. Holzmann “Coupled Electron-Ion Monte Carlo Calculations of Dense Metallic Hydrogen”, *Phys. Rev. Lett.* **93**, 146402 (2004).
4. M. Holzmann, C. Pierleoni and D.M. Ceperley, “Zero-point energy of atomic hydrogen by Coupled Electron-Ion Monte Carlo Method”, *Computer Physics Communications* **169**, 421 (2005).
5. C. Pierleoni and D.M. Ceperley: “Computational Methods in Coupled Electron-Ion Monte Carlo”, *CHEMPHYSICHEM* **6**, 1872-1878 (2005).
6. C. Pierleoni and D.M. Ceperley: “The coupled Electron-Ion Monte Carlo method”, *Lecture Notes in Physics*, vol 703, pp 641-683.
7. K. Delenay, C. Pierleoni and D.M. Ceperley: “Quantum Monte Carlo Simulation of the High-Pressure Molecular-Atomic Crossover in Fluid Hydrogen”, *Phys. Rev. Letts.* **97**, 235702 (2006).

VMC vs RQMC

$$r_s=1.31, N_p=N_e=16, \theta=2\pi(0.4,0.5,0.6)$$

fixed pair of protonic configurations, 1000 blocks of 40000 esteps



$$E_{RQMC} - E_{VMC} = 5.7mH/at = 1810K/at$$

Metallic Hydrogen: VMC vs RQMC

$r_s=1.2$, $T=5000\text{K}$, $N_p=54$, zero phase.

- RQMC gives total energy lower by $7.6(2)\text{mH/at}=2400(60)\text{K/at}$
- RQMC pressure is 0.03Mbars lower than VMC (0.5%)

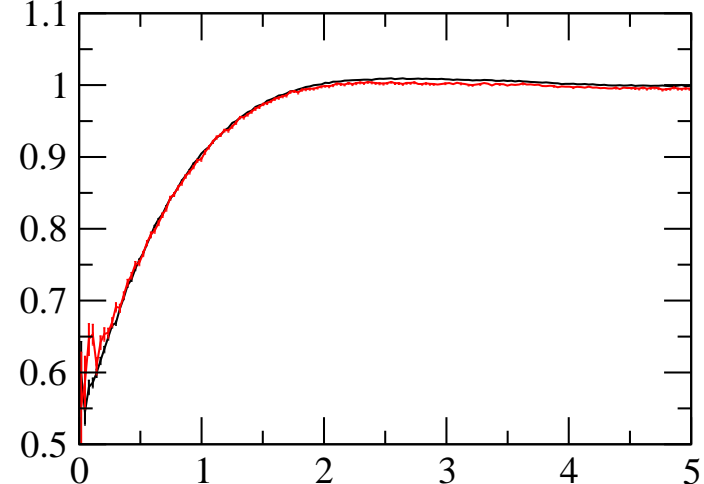
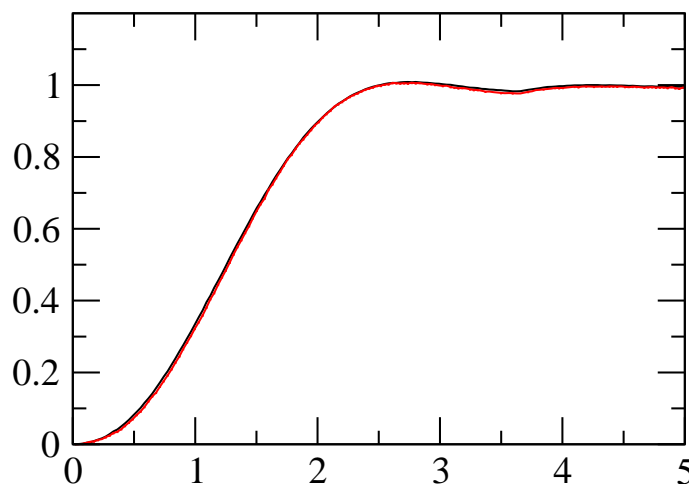
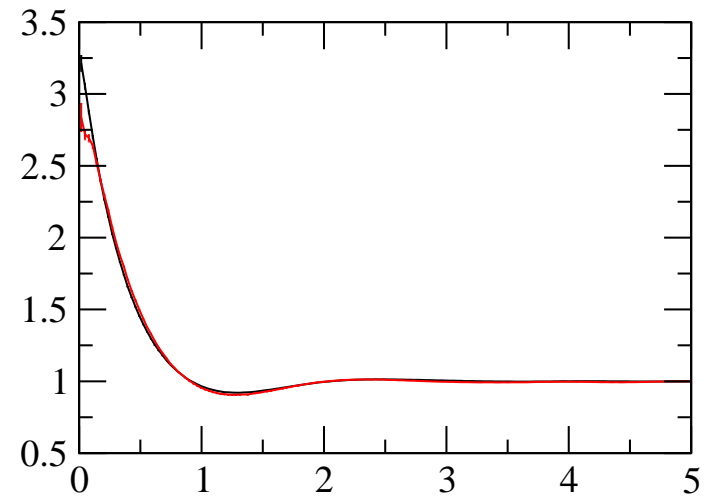
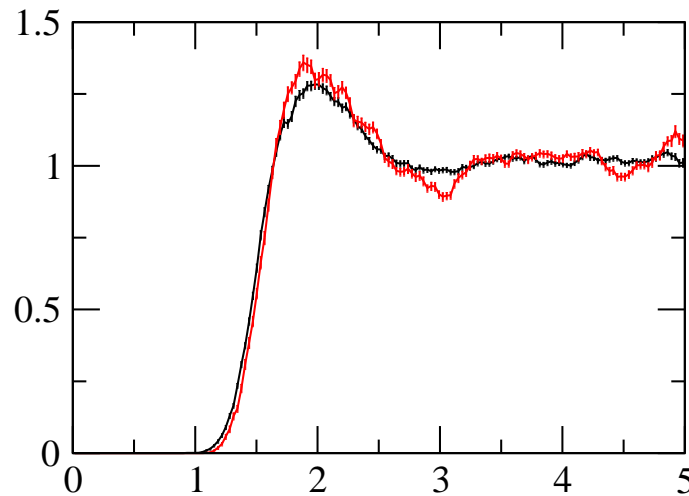
τ_e	$E_{tot}(\text{h/at})$	σ^2	E_{kin}	E_{pot}	P (Mbars)
vmc	-0.4694(2)	0.0472(4)	0.8812(4)	-1.3508(4)	5.55(1)
0.01	-0.4768(4)	—	0.8850(6)	-1.3618(6)	5.50(1)
0.00	-0.47696	—	0.89112	-1.36808	5.581

- CPU time for RQMC $\simeq 10 \times$ (CPU time for VMC)

Metallic Hydrogen: VMC vs RQMC

$r_s=1.2$, $T=5000\text{K}$, $N_p=54$, zero phase

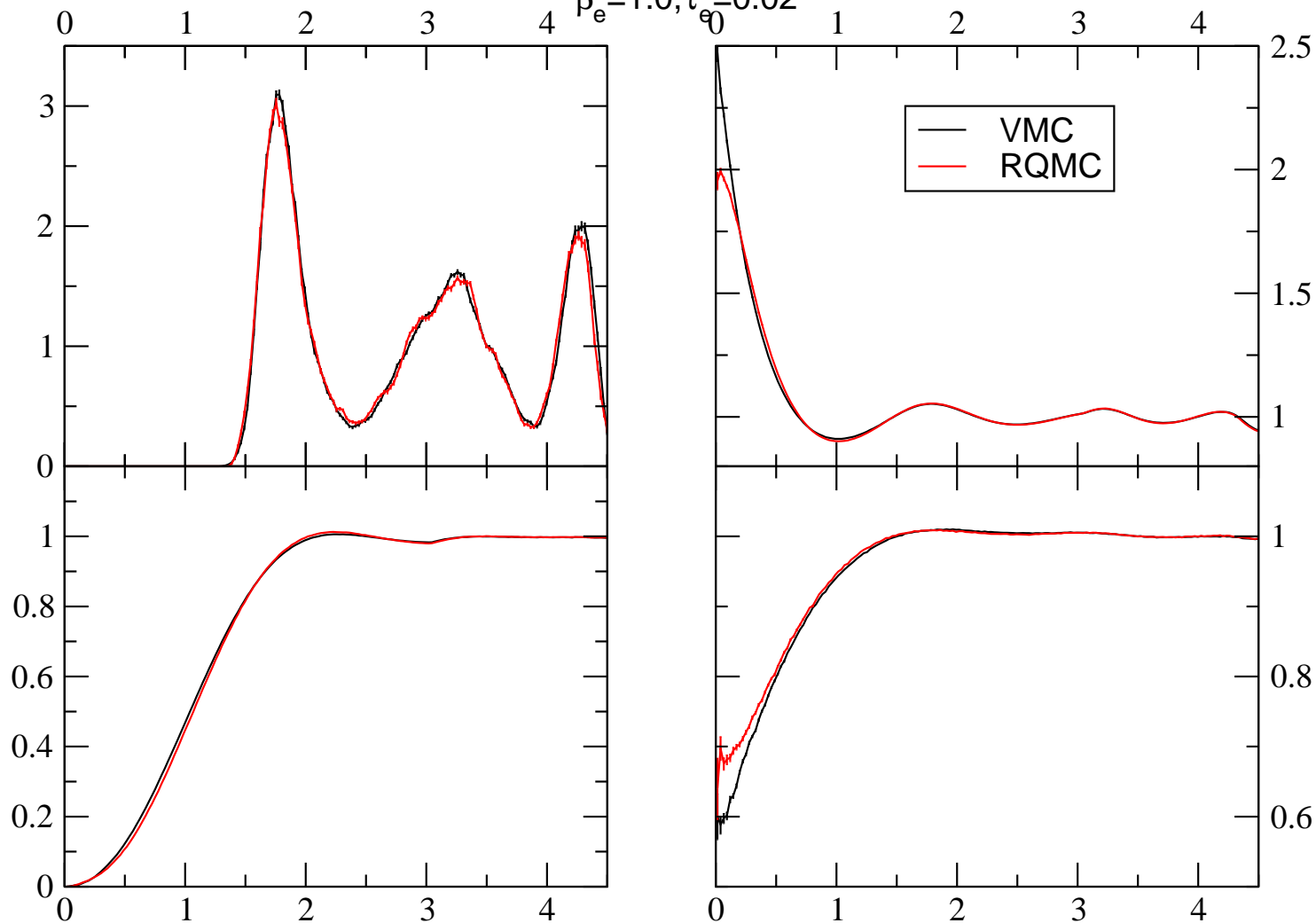
— VMC
— RQMC



Metallic Hydrogen: VMC vs RQMC

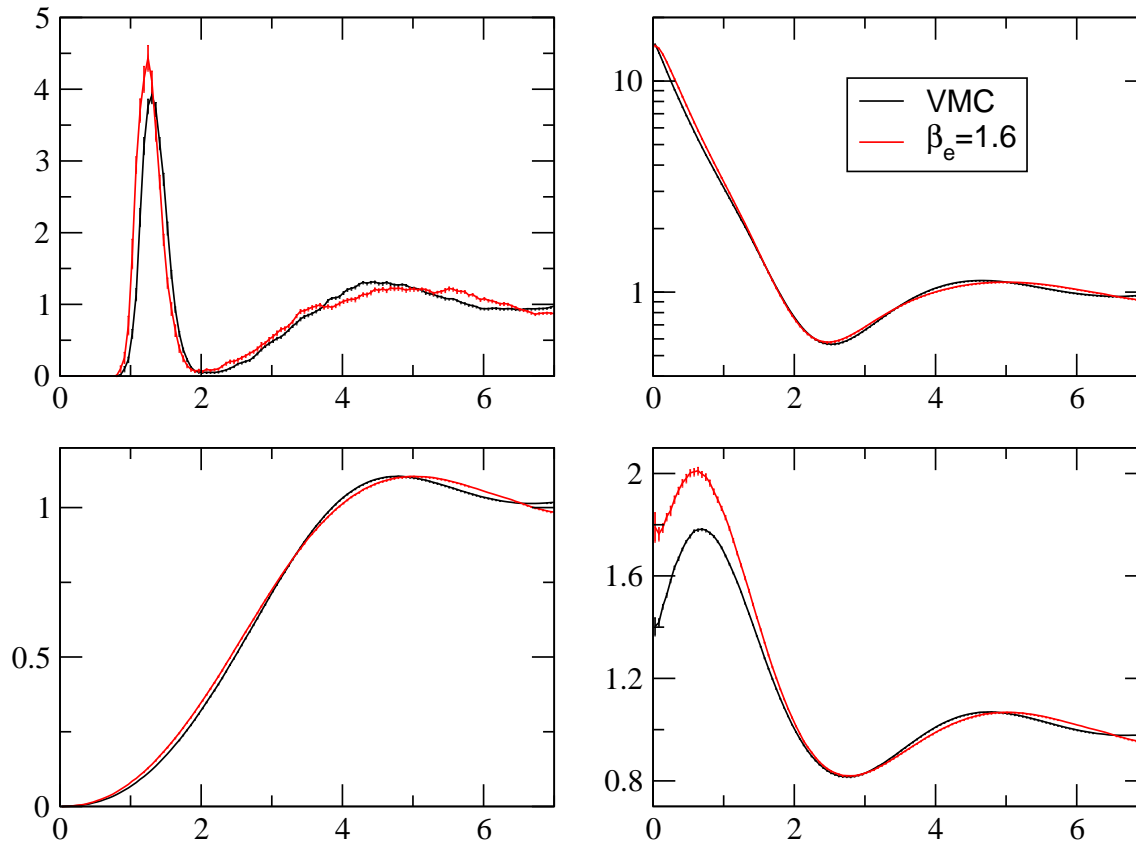
$R_s=1, T=1000\text{K}, N_p=54, \Gamma$ point

$\beta_e=1.0, \tau_{e0}=0.02$



Insulating Molecular Hydrogen

$r_s=2.1$, $T=4.53\text{K}$, $N_p=54$

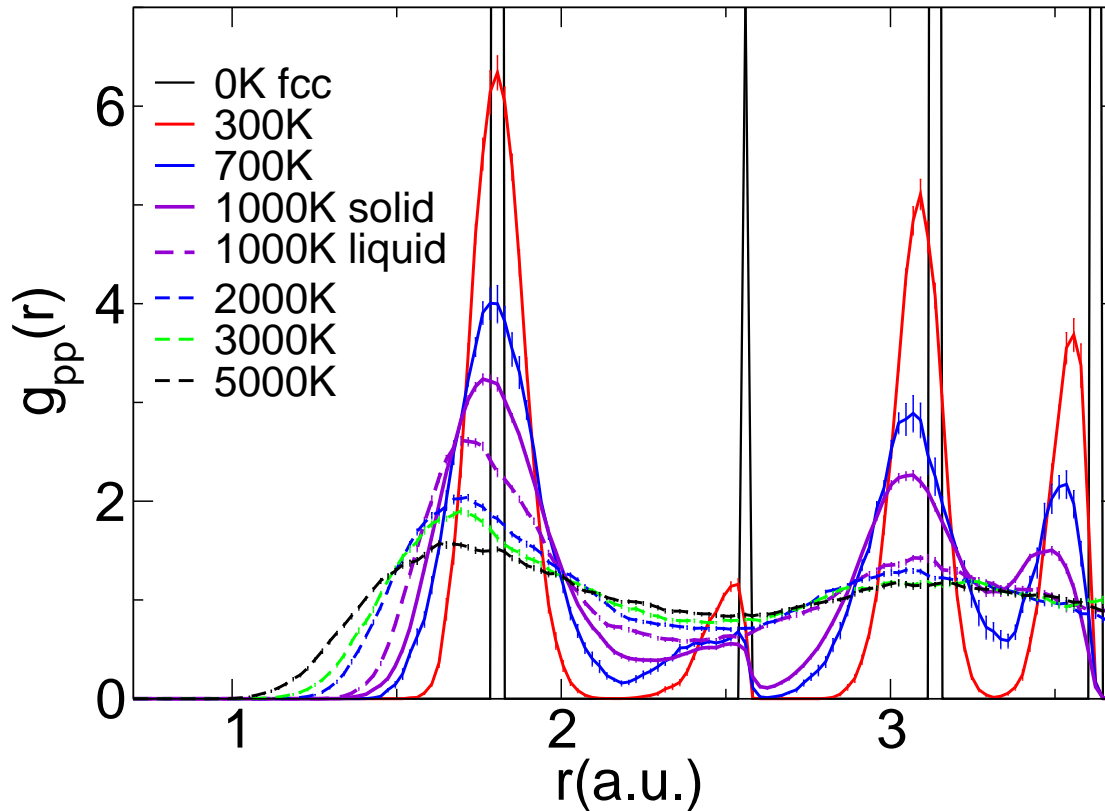


LCAO: one gaussian center on each proton of the molecule. A single variational parameter

$P_{VMC}=0.149(2)\text{Mbars}$, $P_{RQMC}=0.224(5)\text{Mbars}$, $P_{gas-gun}=0.234\text{Mbars}$

We still don't have quantum protons here ! sorry

Atomic Metallic Hydrogen



$r_s = 1, N_e = N_p = 32$ spin unpolarized. Temperature dependence of the proton-proton pair correlation functions for classical protons. The difference between the crystal and the liquid is clearly seen. Melting temperature is between 1000K and 1500K.